Propellants, Explosives, Pyrotechnics

DOI: 10.1002/prep.202000220

Insensitive High Explosives: V. Ballistic Properties and Vulnerability of Nitroguanidine Based Propellants

Ernst-Christian Koch*[a]

Dedicated to Professor Dr. Thomas M. Klapötke on the occasion of his 60th birthday

Abstract: This paper reviews the ballistic properties, stability and vulnerability of gun propellants, gas generators and rocket propellants containing nitroguanidine (NGu), CAS–No [556-88-7] as an energetic filler. Nitroguanidine and its formulations burn stable over a broad pressure regime extending from subatmospheric to high pressures (0.1 kPa–400 MPa). Its high nitrogen content (53.83 %) and oxygen balance (Ω =-30.75 %) effects a high gas pressure in gun propellants combined with low explosion temperature and consequently low signature and reduced erosion. NGu is an effective stabilizer for a broad array of energetic materials encountered in gun and rocket propellants including AP, ADN, HMX, RDX, NGl and also materials with low thermal stability such as NC, HNF, TNAZ and ADN. Finally, the low vulnerability of NGu-based propellant formulations makes them taylor made to serve insensitive munitions. This review covers 31 NGu-based rocket and gas generating propellant formulations, 44 gun propellants, five of which contain guanylurea dinitramide, (GuDN, FOX-12), CAS–No [217464-38-5] for comparison, four reference propellants containing neither of the aforementioned ingredients and six combustible cartridge case formulations based on NGu. In addition, the combustion properties of pure NGu, pure GUDN and NGu modified with 17 different catalysts are revised. The review contains 142 references from the public domain.

Keywords: Nitroguanidine · Combustion · Guanylurea dinitramide · Gun Propellants · Rocket Propellants · Vulnerability

1 Introduction

Nitroguanidine (NGu) (Figure 1) is an available, inexpensive, sustainable energetic material that thanks to its energy content and due to its extreme low sensitiveness [1] fulfils multiple roles as high explosive [2], ingredient in gun and missile propellants and pyrotechnics. Though it has been in use as an energetic filler in gun propellants for over 100 years and has been used intensively in missile propellants and similar applications for over 50 years there lacks a contemporary review of its combustion and deflagration properties and the vulnerability of the corresponding formulations. Thus, nitroguanidine has occasionally been overlooked as an ingredient in advanced, insensitive and low erosion propellants [3]. It is therefore the purpose of the present paper to review and consolidate performance and sensitivity information on the use of nitroguanidine in all kinds of propellant applications (gun, missile, base bleed, gas generator).

As a courtesy for the reader nitroguanidine will be compared with available data on guanylurea dinitramide (FOX-12, GUDN) (Figure 1, right), a material that has quite similar properties (density, sensitiveness, performance) and which entered the market in the late 1990s. Table 1 presents a synopsis of the pertinent properties of both nitroguanidine and guanylurea dinitramide.

2 Combustion and Deflagration

2.1 Pure Nitroguanidine

Nitroguanidine is capable of deflagration in the absence of oxygen in accordance with the following formal equation:

$$CH_4N_4O_2 \rightarrow H_2 + H_2O_{(l)} + 2\,N_2 + CO,\ \Delta_RH = -296.2\ \mathrm{kJ\,mol^{-1}} \qquad (1)$$

which is supported by thermochemical equilibrium calculations (Table 2 and Table 3) using NASA-CEA.

No experimental data on the chemical composition of the deflagration products of nitroguanidine have been reported so far. Hence the decomposition products from fast heating of NGu are the only data which can be used remotely to estimate the composition of the deflagration products [4]. Figure 2 shows the composition products of spherical high bulk density NGu as a function of heating temperature. Unlike the calculated deflagration composition, N_2O (63 Vol-%), NH_3 (30 Vol-%), CO_2 (5 Vol-%) account

[a] *E.-C. Koch*
Lutradyn Energetic Materials
Burgherrenstraße 132
67661 Kaiserslautern
**e-mail: e-c.koch@lutradyn.com*

 © 2021 Wiley-VCH GmbH

Table 1. Pertinent physical and thermochemical properties of Nitroguanidine and FOX-12.

Property	Unit	NGu (I)	FOX-12 (GUDN) (II)
CAS–No.		[556–88–7]	[217464–38–5]
EINECS		209-143-5	
UN-Number		1336*	
Formula		$CH_4N_4O_2$	$C_2H_7N_7O_5$
Ω	wt.-%	−30.75	−19.13
N	wt.-%	53.83	46.87
m_r	$g\,mol^{-1}$	104.068	209.121
ρ at 298 K	$g\,cm^{-3}$	1.77	1.76
$\Delta_f H$	$kJ\,mol^{-1}$	−98.74	−356
Mp	°C	257 (dec.)	215
T_{dec}	°C	254	
$\Delta_{ex}H$	$kJ\,mol^{-1}$	−405.7	−792.2
	$kJ\,g^{-1}$	−3.898	−3.789
	$kJ\,cm^{-3}$	−6.857	−6.667
c_p	$J\,g^{-1}K^{-1}$	1.198	
c_L	$m\,s^{-1}$	3350	
κ	$W\,m^{-1}K^{-1}$	4.1 10^{-3}	
$S(H_2O)$ at 25 °C	$g\,kg^{-1}$	3.45	3.4 at 20 °C
ARC	°C	159, $\phi=5.82$	163, $\phi=8.3$
V_D	$m\,s^{-1}$	8344#	7966
P_{CJ}	GPa	29.0#	26.1
$\sqrt{2E_G}$	$m\,s^{-1}$	2435#	
Impact	J	>50	<50
Friction	N	>355	>355

*) (for NGu wetted with >20 wt.-% H_2O).
#) AFX-902 (95 wt.-% NGu, 5 wt.-% Viton®A) at $\rho=1.742\,g\,cm^{-3}$.

for 98 Vol-% of the pyrolysis products and minor traces of NO, N_2 and HCN.

The combustion of NGu under inert gas has been studied experimentally in the pressure range between 0.1–100 MPa. The adiabatic equilibrium temperature composition for the deflagration of NGu, has been calculated using NASA-CEA Code at constant pressure (p=0.01, 0.1, 1, 10, 100, 500 MPa) [5] (see Table 1 and 2).

Glazkova has investigated the burning rate of NGu with and without combustion catalysts up to pressures of 100 MPa under nitrogen. Figure 3 shows the burning rate of pure NGu and in the presence of twelve different catalysts [6–8]. NGu burns at ambient pressure at the very low rate of $u=0.1\,mm\,s^{-1}$. In the presence of V_2O_5, the combustion rate speeds up to $u=0.6\,mm\,s^{-1}$. While V_2O_5 yields the highest burning rates up to pressures around 10 MPa, CuCl effects the highest burning rate in the high pressure-regime up to 100 MPa with a 2.2 times higher burning rate compared to pure NGu (u(NGu)100 MPa = 24.5 $mm\,s^{-1}$).

$$u = a \cdot p^n \tag{2}$$

Table 4 displays the Vieille coefficients a and n for pure NGu and NGu with various additives at 5 wt-%-level in different pressure regimes.

Fogel'zang et al. have studied the combustion rate of NGu at higher charge density ($\rho=1.7\,g\,cm^{-3}$) and found an overall lower combustion rate compared to low-density

Table 2. Adiabatic Equilibrium Composition and temperature at various pressures for NGu.

Parameter	MPa	0.1	0.5	1	5	10	50	100	500
Temperature	K	1807	1808	1808	1808	1808	1813	1823	1900
γ	–	1.2685	1.2698	1.2701	1.2704	1.2703	1.2681	1.2635	1.2431
M_w	$g\,mol^{-1}$	20.812	20.813	20.813	20.816	20.819	20.861	20.942	21.570
CH_4	Mol-%	0.00000	0.00000	0.00000	0.00001	0.00003	0.00060	0.00205	0.01454
CO	Mol-%	0.16822	0.16825	0.16825	0.16825	0.16824	0.16775	0.16654	0.15559
CO_2	Mol-%	0.03176	0.03175	0.03174	0.03175	0.03177	0.03200	0.03245	0.03632
H	Mol-%	0.00018	0.00008	0.00006	0.00003	0.00002	0.00001	0.00001	0.00000
HCN	Mol-%	0.00000	0.00000	0.00000	0.00001	0.00001	0.00007	0.00013	0.00044
HNCO	Mol-%	0.00000	0.00000	0.00000	0.00000	0.00000	0.00001	0.00003	0.00012
H_2	Mol-%	0.23165	0.23168	0.23168	0.23158	0.23141	0.22905	0.22447	0.18935
H_2O	Mol-%	0.16821	0.16824	0.16825	0.16828	0.16832	0.16912	0.17096	0.18599
NH_3	Mol-%	0.00000	0.00001	0.00002	0.00010	0.00020	0.00099	0.00189	0.00638
N_2	Mol-%	0.39996	0.39998	0.39999	0.39999	0.40000	0.40038	0.40144	0.41106

Table 3. Cooled Equilibrium Composition at various pressures for adiabatic combustion of NGu.

Parameter	MPa	0.1	0.5	1	5	10	50	100	500
Temperature	K	300	300	300	300	300	300	300	300
CH_4	Mol-%	0.00127	0.00025	0.00012	0.00002	0.00001	0.00000	0.00000	0
CO_2	Mol-%	0.00127	0.00025	0.00012	0.00002	0.00001	0.00000	0.00000	0
H_2O	Mol-%	0.01478	0.00285	0.00142	0.00028	0.00014	0.00003	0.00001	0
N_2	Mol-%	0.40102	0.40020	0.40010	0.40002	0.40001	0.40000	0.40000	0.4
C(gr)	Mol-%	0.19796	0.19961	0.19980	0.19996	0.19998	0.20000	0.20000	0.2
$H_2O(L)$	Mol-%	0.38369	0.39685	0.39843	0.39969	0.39984	0.39997	0.39999	0.4

© 2021 Wiley-VCH GmbH

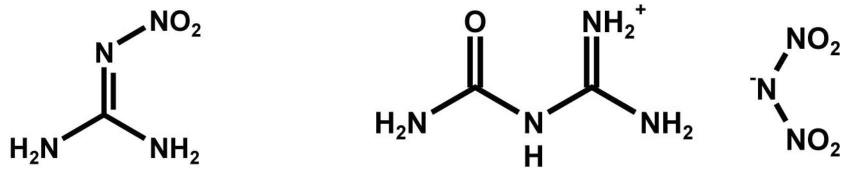

Figure 1. Structure of nitroguanidine (NGu) (**I**) and guanylurea dinitramide (GUDN, FOX-12) (**II**).

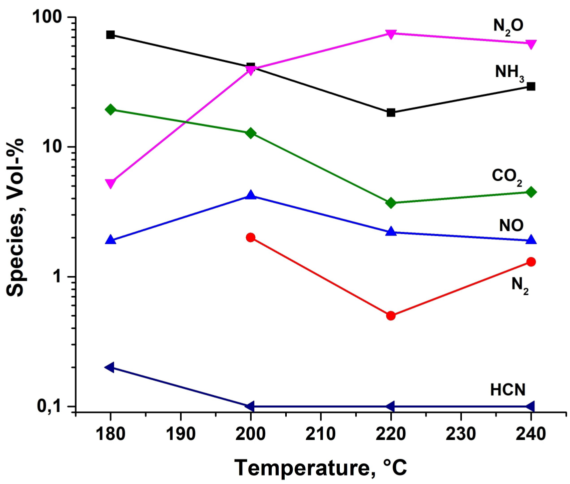

Figure 2. Decomposition gases of NGu as function of pyrolysis temperature after *Volk et al.* [4].

NGu ($\rho = 1.0\ \mathrm{g\,cm^{-3}}$) as is depicted in Figure 4. The same graph also shows the burning rate for low density ($\rho <$ $1\ \mathrm{g\,cm^{-3}}$) FOX-12 ($u = 1.337{\cdot}p^{0.754}$) indicating a similar combustion behavior [9]. It is evident from the position of the data points for high-density NGu (open squares) in Figure 4 that the pressure dependence of high-density NGu does not follow a simple Vieille-type law but that pressure sensitivity of combustion varies with pressure itself. The burning rate of low-density FOX-12 is in the same ballpark as for NGu but shows a greater pressure exponent. The combustion of pure high-density FOX-12 on the other hand is insufficiently slow to support any use as a gas generator [10].

2.2 NGu-Oxidizer Formulations

2.2.1 Nitroguanidine/Ammonium Nitrate

Nitroguanidine is one of the very few fuels (among charcoal and others) to yield stable combustion with ammonium nitrate as the sole oxidizer at ambient pressure [8]. NGu/AN systems have therefore been suggested as a gas generating composition for base bleed units and also vehicle restraint systems [11,12]. *Glazkova* investigated the burning rate of

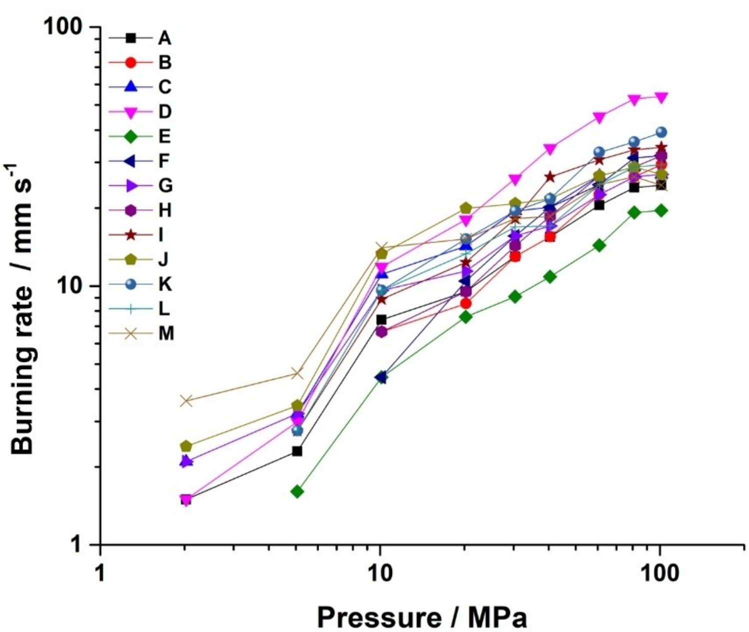

Figure 3. Pressure dependent burning rate of NGu ($\rho \sim 1.0\ \mathrm{g\,cm^{-3}}$) with and without catalysts (5 wt.-%) A = pure NGu, B = $Co(NO_3)_2{\cdot}6\ H_2O$, C = Cu, D = CuCl, E = Fe-catechol, F = KBr, G = $K_2Cr_2O_7$, H = NaCl, I = $PbCl_2$, J = $PbCrO_4$, K = $PbCrO_4$ + CuCl, L = PbO + Cr_2O_3 + CuCl, M = V_2O_5.

© 2021 Wiley-VCH GmbH

Table 4. Vieille coefficients for NGu and with various additives at 5 wt-% level from [6–8].

Additive	Pressure Range (MPa)	a ($mm\,s^{-1}$)	n (−)
NGu	0.1–60	0.11	0.835
	65–100	8.71	0.15
$Co(NO_3)_2 \cdot 6\ H_2O$	10–50	0.046	0.966
	50–100	1.16	0.457
Cu	5–50	0.31	0.647
	55–90	7.24	0.202
$Cu_5H_8[B(W_2O_7)_6]_2 \cdot 36\ H_2O$	5–100	0.12	0.8
CuCl	2–60	0.09	0.0974
	65–100	6.51	0.311
CuC_2O_4	7–100	0.096	0.818
$CuC_{14}H_{10}O_6$	5–100	0.034	1.01
$Fe[C_6H_4(OH)_2]_3$	5–100	0.096	0.787
KBr	5–80	0.06	0.927
	80–100	8.73	0.188
$K_2Cr_2O_7$	5–30	0.14	0.806
	30–100	0.60	0.56
NaCl	5–70	0.085	0.887
	70–100	0.84	0.53
$NaC_7H_5O_3$	10–60	0.02	1.135
	60–100	1.2	0.5
$PbC_{14}H_{10}O_4$	5–40	0.43	0.982
	40–100	0.37	0.659
$PbCl_2$	5–35	0.05	1.05
	40–100	9.38	0.187
$PbCrO_4$	0.1–40	0.21	0.775
	40–80	2.57	0.361
$PbCrO_4 + CuCl$	5–70	0.19	0.79
	70–100	5.73	0.276
$PbO + Cr_2O_3 + CuCl$	5–80	0.23	0.724
V_2O_5	2–100	0.62	0.578

Table 5. Vieille coefficients for AN/NGu with various additives at 5 wt-% level from [7].

Additive	Pressure Range (MPa)	a ($mm\ s^{-1}$)	n (−)
NGu	0.1–60	0.11	0.835
	65–100	8.71	0.15
AN/NGu (61/39)	0.1–25	0.2	0.824
	50–100	0.35	0.656
AN/NGu/CuCl (54/41/5)	0.1–40	1.2	0.56
	60–100	0.5	0.656
AN/NGu/$K_2Cr_2O_7$ (54/41/5)	0.1–50	1.1	0.596
	50–100	9.8	0.249
AN/NGu/KNO_3 (54/41/5)	1–50	2.6	0.433

stoichiometric mixtures of ammonium nitrate with NGu (2 NH_4NO_3/ 1 $CH_4N_4O_2$ = 61/39 wt-%) with additives (5 wt-%) and without (Table 5/Figure 5). AN/NGu CuCl yields the highest burning rate up to pressure of 20 MPa while $K_2Cr_2O_7$ effects the highest burning rates at pressures around 100 MPa. The combustion rate law for various NGu/AN mixtures has been studied in Ref. [13].

Table 6 and 7 show the adiabatic combustion temperature and equilibrium composition at assigned temperature for NGu/AN 39/61. As the composition does not change appreciably, the temperature does not change very much either ($\Delta T = 153$ K).

Blomquist has studied the combustion properties (Figure 6) of a fuel rich formulation containing 60 wt.-% NGu and 40 wt.-% AN [14]. This formulation is both friction (> 355 N) and impact insensitive (> 50 J) when tested in the corresponding BAM-machines.

The ambient pressure (p = 0.1 MPa) burning rate of ammonium nitrate/FOX-12 (60/40) is u = 0.1 mm/s [15].

2.2.2 Nitroguanidine/Potassium Nitrate

Engelen and *Lefebvre* have investigated NGu/KNO_3 (55/45) as a propellant system [16–19]. The NGu applied in this study was needle-like low bulk density NGu (2×2×20–25 μm). They found that with an increasing particle size (reduction in specific surface area) of KNO_3

- the ignition delay increases,
- the burning rate (Figure 7) and dynamic vivacity decrease, and
- the yield of cooled gas increases.

Similar as with AN/NGu based on thermochemical calculations the effect of pressure on the combustion of KNO_3/NGu has only negligible effect ($\Delta T = 156$ K) (Table 8 and 9).

2.2.3 Nitroguanidine/Strontium Nitrate

Cao et al. have investigated the influence of NGu on a propellant (Table 10) based on 5-aminotetrazole and strontium nitrate [20]. NGu yields a pronounced *mesa*-effect in the pressure range between 4.9–5.4 MPa (Figure 8).

2.2.4 Nitroguanidine/Ammonium Perchlorate

2.2.4.1 Rocket Propellant Applications

NGu/ammonium perchlorate/binder was used in the slow-burning sustainer-propellant, **ANP-2874** [21] of both legacy RIM-24 (Tartar missile) and its immediate successor RIM-66B (Standard Missile), as well as in the formulation **ANP-3196** which was used in both, legacy AGM-45 (Shrike missile), AGM-123 (Skipper missile), and continues to be in use with the MIM-23B (improved Hawk-Surface-to-Air Missile) [22]. Table 11 shows the overall composition of both grains [23] and the published compositional details of AP/NGu/Binder systems. Table 12 depicts the experimentally determined and calculated performance [24–26].

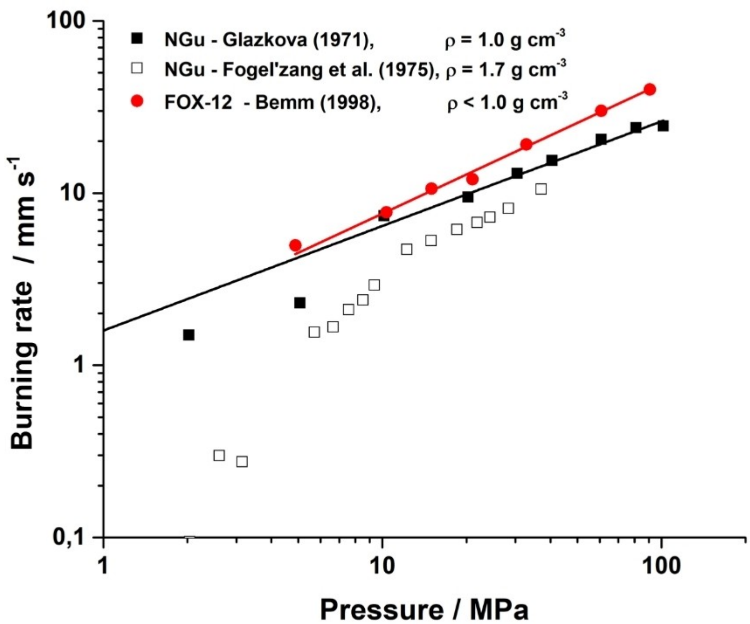

Figure 4. Pressure dependent burning rate of NGu at low and high density and low-density FOX-12.

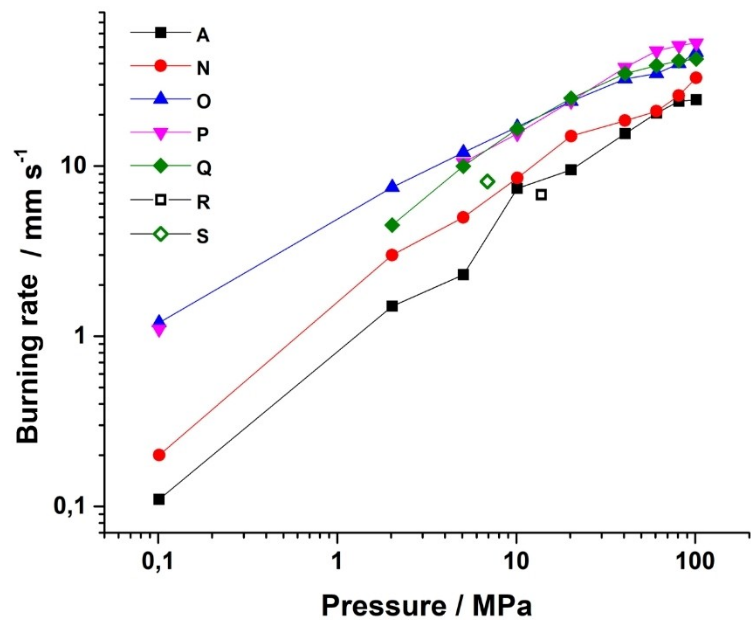

Figure 5. Pressure dependent burning rate of AN/NGu (61/39)(ρ ~ 1.0 g cm^{-3}) with and without catalysts (5 wt-%) [13] A = pure NGu, N = AN/NGu(61/39), O = AN/NGu/CuCl (54/41/5), P = AN/NGu/$K_2Cr_2O_7$(54/41/5), Q = AN/NGu/KNO_3(54/41/5), R = AN/NGu(70/30), S = AN/NGu (75/25).

Figure 9a displays the calculated specific impulse for the ternary propellant containing NGu-AP-HTPB (top left). Replacing ammonium perchlorate with ammonium dinitramide (ADN) and substituting glycidyl azide polymer (GAP) for HTPB (Figure 9b, bottom left) not only yields a better tactical signature (AA vs AC) [28] but also affords a higher performance (+30 s). A comparison between NGu and FOX-12 (Figs 9c and d) reveals that no appreciable effects are obtained as is seen from the practically identical I_{sp}-plots. The color scales fit the minimum and maximum I_{sp} for each system and hence vary considerably between the ammonium perchlorate and the ammonium dinitramide-based systems.

© 2021 Wiley-VCH GmbH

Table 6. Adiabatic Equilibrium Composition and temperature at various pressures for NGu/AN 39/61.

Parameter	MPa	0.1	0.5	1	5	10	50	100	500
Temperature	K	2315	2365	2383	2417	2429	2450	2456	2468
γ	–	1.1468	1.1592	1.1643	1.1754	1.1796	1.1879	1.1908	1.1961
M_w	$g\,mol^{-1}$	23.651	23.755	23.793	23.866	23.890	23.934	23.948	23.971
CO	Mol-%	0.01032	0.00760	0.00654	0.00439	0.00363	0.00223	0.00177	0.00099
CO_2	Mol-%	0.07832	0.08142	0.08263	0.08504	0.08590	0.08747	0.08798	0.08884
H	Mol-%	0.00115	0.00055	0.00039	0.00017	0.00011	0.00004	0.00003	0.00001
H_2	Mol-%	0.01214	0.00850	0.00717	0.00465	0.00379	0.00227	0.00179	0.00099
H_2O	Mol-%	0.52052	0.52800	0.53073	0.53590	0.53766	0.54078	0.54177	0.54343
NO	Mol-%	0.00230	0.00217	0.00209	0.00186	0.00176	0.00153	0.00144	0.00126
N_2	Mol-%	0.35636	0.35800	0.35862	0.35982	0.36024	0.36101	0.36127	0.36171
O	Mol-%	0.00052	0.00026	0.00019	0.00009	0.00006	0.00002	0.00002	0.00001
OH	Mol-%	0.00903	0.00669	0.00578	0.00398	0.00335	0.00220	0.00182	0.00117
O_2	Mol-%	0.00934	0.00679	0.00586	0.00409	0.00349	0.00243	0.00210	0.00155

Table 7. Cooled Equilibrium Composition at various pressures for adiabatic combustion of NGu/AN.

Parameter	MPa	0.1	0.5	1	5	10	50	100	500
Temperature	K	300	300	300	300	300	300	300	300
CO_2	Mol-%				0.08995				
H_2O	Mol-%	0.01664	0.00323	0.00161	0.00032	0.00016	0.00003	0.00002	0
N_2	Mol-%				0.36281				
O_2	Mol-%				0.00151				
$H_2O(L)$	Mol-%	0.52909	0.54250	0.54412	0.54541	0.54557	0.54570	0.54571	0.54573

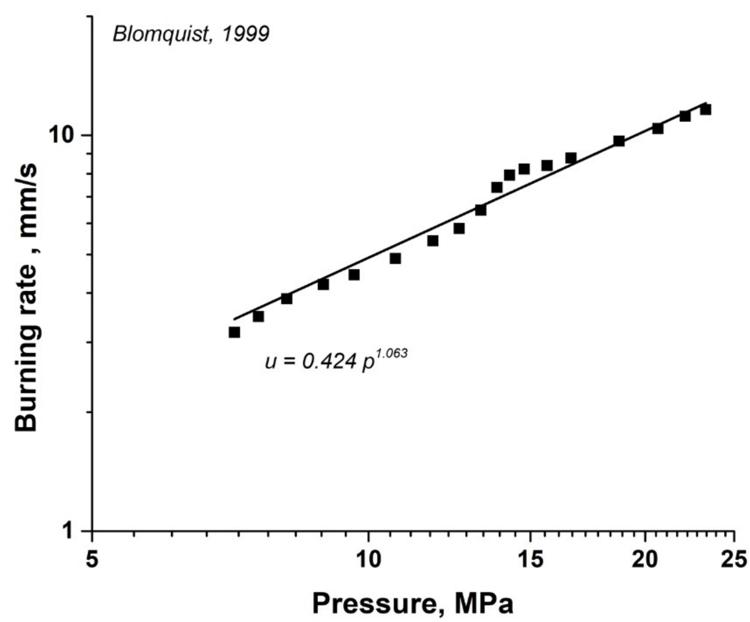

Figure 6. Pressure dependent burning rate of AN/NGu (40/60)(ρ ~ 1.5 $g\,cm^{-3}$) after *Blomquist*, 1999 [14].

Liljedahl et al. calculated the performance and tested the mechanical sensitivity of GAP-based propellant formulations (Table 13) using co-prilled ADN/FOX-12 [29]. While pure FOX-12 is practically insensitive to impact and friction (Table 1), its formulation with GAP yields friction insensitive and just mildly impact sensitive formulation (**9**). However, successive replacement by ammonium dinitramide yields both increasing friction and most importantly increasing impact sensitivity that reaches the level of pure un-phlegmatized PETN (3.3 J) at 70 wt.-% ADN [30,31].

© 2021 Wiley-VCH GmbH

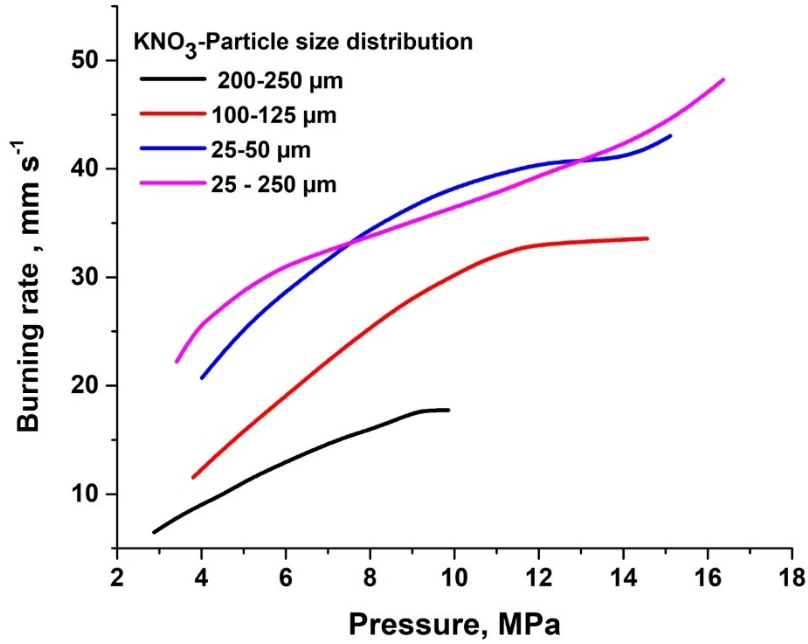

Figure 7. Burning rate of KNO_3/NGu as a function of KNO_3-particle size and pressure [16–19].

Table 8. Adiabatic Equilibrium Composition and temperature for NGu/KNO_3 55/45 [5].

Parameter	MPa	1	2.5	5	10	15	20
Temperature	K	2084	2099	2112	2153	2201	2240
γ	–	1.1887	1.1922	1.1934	1.1644	1.0625	1.1754
M_w	g mol^{-1}	32.043	32.144	32.250	32.463	32.323	32.244
CO	Mol-%	0.00142	0.00104	0.00083	0.00078	0.00090	0.00102
CO_2	Mol-%	0.16788	0.16875	0.16946	0.16670	0.16879	0.16926
H_2	Mol-%	0.00046	0.00034	0.00026	0.00025	0.00027	0.00030
H_2O	Mol-%	0.26765	0.26821	0.26904	0.27462	0.27035	0.26857
K	Mol-%	0.00258	0.00140	0.00087	0.00057	0.00043	0.00034
KOH	Mol-%	0.13666	0.13441	0.13006	0.11857	0.09605	0.07924
$(KOH)_2$	Mol-%	0.00151	0.00340	0.00601	0.00843	0.00699	0.00555
NO	Mol-%	0.00145	0.00147	0.00150	0.00165	0.00183	0.00198
N_2	Mol-%	0.40924	0.41052	0.41184	0.41447	0.41259	0.41150
OH	Mol-%	0.00144	0.00121	0.00107	0.00108	0.00117	0.00125
O_2	Mol-%	0.00932	0.00884	0.00859	0.00844	0.00832	0.00825
KOH(L)	Mol-%	0.00000	0.00000	0.00000	0.00000	0.03083	0.05228
K_2CO_3(L)	Mol-%	0.00000	0.00000	0.00000	0.00388	0.00097	0.00000

Table 9. Cooled Equilibrium Composition for adiabatic combustion of NGu/KNO_3 55/45 [5].

Parameter	MPa	1	2.5	5	10	15	20
Temperature	K	300	300	300	300	300	300
CO_2	Mol-%	0.11025					
H_2O	Mol-%	0.00195	0.00078	0.00039	0.00019	0.00013	0.00010
N_2	Mol-%	0.44100					
$H_2O_{(L)}$	Mol-%	0.36555	0.36672	0.36711	0.36731	0.36737	0.36740
$KNO_{3(s)}$	Mol-%	0.00775					
$K_2CO_{3(s)}$	Mol-%	0.07350					

© 2021 Wiley-VCH GmbH

Table 10. Vieille coefficients for 5-AT/$Sr(NO_3)_2$ with and without added NGu [20].

Composition	Pressure Range (MPa)	*a* ($mm\,s^{-1}$)	*n* (−)
5-AT/$Sr(NO_3)_2$: 36.42/63.58	2.8–7	5.54	1.36
5-AT/$Sr(NO_3)_2$/NGu: 29.83/60.17/10	2.8–7	11.58	1.22
	4.9–5.4 (mesa)	160.61	−0.22

Table 11. Overall missile sustainer compositions containing AP/NGu/Binder [21–26].

	Unit	ANP-2874*)	ANP-3196
Nitroguanidine	wt-%	X	15-20
Ammonium perchlorate	wt-%	X	60-75
Polyurethane	wt-%	X	
Nitrated Polymer	wt-%	X	
Isodecyl pelargonate	wt-%		X
Polyglycol	wt-%		X

*) solid fill grade of approximately 70% vol-% [27].

Performance calculations of aluminized NGu-AP-HTPB for a range of stoichiometries have been reported by *Hadhoud et al.* [32]. Other rocket propellants based on AP/NGu/silicone binder have been suggested in Ref. [33]. A Chinese research paper has focused on the effect of FOX-12 content on AP/HTPB/Al [34].

Li and Wang have used highly resolved FTIR to characterize the ambient pressure combustion plume of a solid grain consisting of nitroguanidine, "(…) *a large quantity of ammonium perchlorate* (…)" and polytetrafluoroethylene (PTFE) [35]. The plume temperature has been determined by rotational analysis of the HCl bands. Though an exact stoichiometry was not given by authors, the temperature, 1916 K, and the volumetric concentration ratio HCl (659 ppm) /HF (286 ppm) ~2.3 indicate a stoichiometry in the overall range: 15–20 wt-% NGu, 75 wt.-% AP and 5–10 wt-% PTFE. Figure 10 depicts the FTIR spectrum of the ambient pressure combustion flame of a bare cylindrical

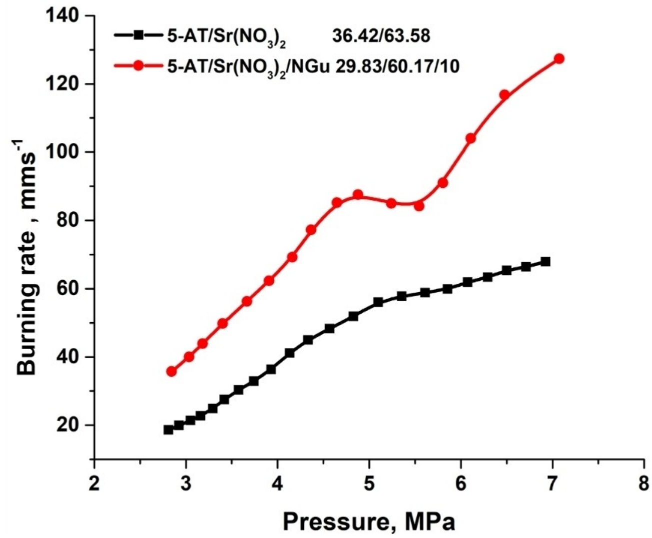

Figure 8. Burning rate of 5-AT/$Sr(NO_3)_2$ with and without additive NGu as a function of pressure [20].

Table 13. Composition performance and sensitiveness of ADN/FOX12/GAP [29].

	Unit	4	5	6	7	8	9
FOX-12	wt.-%	0	7	14	21	28	70
Ammonium dinitramide	wt.-%	70	63	56	49	42	0
GAP	wt.-%	30	30	30	30	30	30
I_{sp} (calc)	s	254	248	242	236	230	196
BAM-Impact Sensitivity	J	3.3	6.1	4.5	7.7	5.3	35-50
BAM-Friction Sensitivity	N	212	292	198	299	270	>360

Table 12. AP/NGu/Binder-formulations [21–26].

	Unit	1	2	3
Nitroguanidine	wt-%	15	17	15
Ammonium perchlorate	wt-%	64	61	50
Polyalkyleneglycole (PAG)	wt-%		11.12	28
Poly-neopentyl glycol azelate (NPGA)	wt-%	21*)		
Hexamethylene diisocyanate,	wt-%			
Ferric acetyl acetonate			10.88#)	
Isodecyl pelargonate				
Nitrocellulose (N content unknown)	wt-%			7
u at 7 MPa and 20 °C	$mm\,s^{-1}$	4		3.81
u at 1.59 MPa and 15.6 °C	$mm\,s^{-1}$		1.27 −1.78	
T_{ad} at 7 MPa	*°C*	*2242*	*2106*	*1593*
I_{sp}	$m\ s^{-1}$	*228*	*224*	*206*

*) total content of unknown ratio of NPGA + HMDI + FA + IDP; #) total content of unknown ratio of HMDI + FA + IDP.

 © 2021 Wiley-VCH GmbH

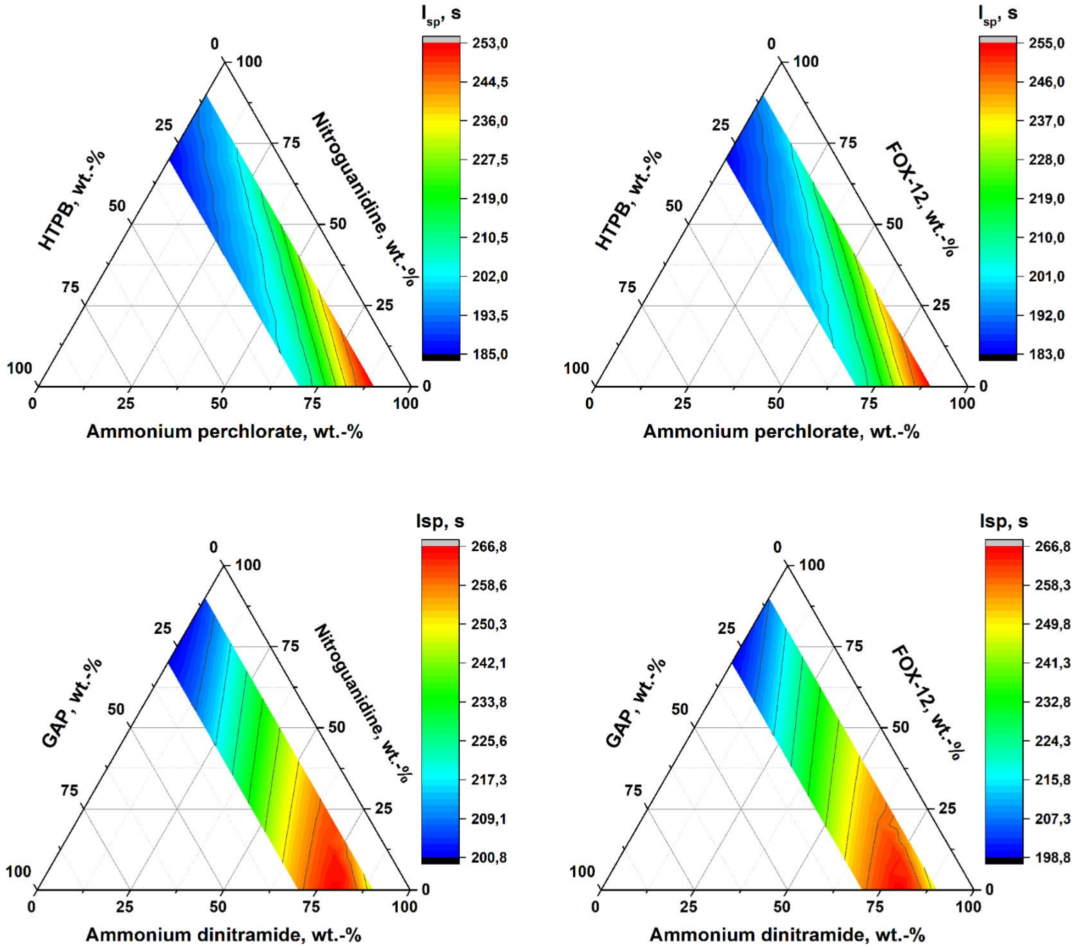

Figure 9. Calculated specific impulse for NGu-AP-HTPB and NGu-ADN-GAP and related formulations containing FOX-12 in place of NGu for an expansion ratio of 70:1 (Note the different color scales).

grain. Ref. [36] describes full scale MIM 23 B-motor burns and subsequent analysis of the combustion products.

ANP-3196 is characterized as a non-detonable propellant [37]. Figure 11 depicts the TNT equivalent overpressure and impulse upon firing a 45 kg charge of **ANP-3196** confined in a steel pipe (diameter = 203 mm, wall thickness 7.94 mm) initiated with a 11 kg Pentolite booster. A 45 kg charge of unconfined TNT with 11 kg Pentolite booster served as a reference.

The IM signatures of two legacy missiles using both **ANP-2874** and **ANP-3196** are depicted in Table 14 [38]. The RIM-66B has a separate booster unit based on a common AP/Al/Binder (similar to formulation **ANP-2969** [39]) attached to the aft end of the main missile body, while the AGM-45 has a concentric dual grain similar to the Hawk missile motor. The latter makes it very hard to distinguish triggering response in either formulation.

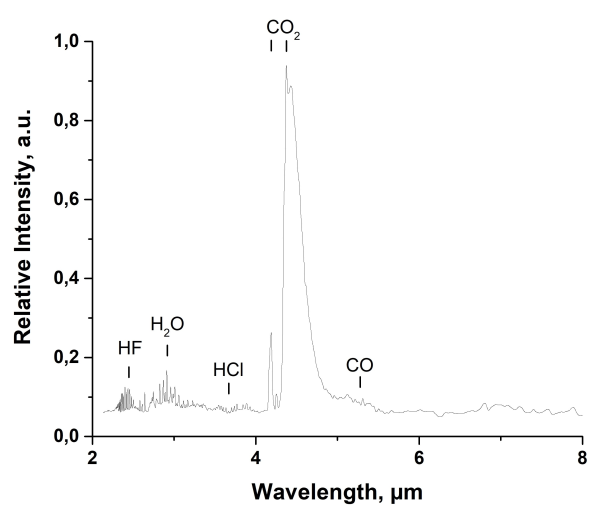

Figure 10. FTIR spectrum of a bare grain burning AP/NGu/PTFE after [35].

© 2021 Wiley-VCH GmbH

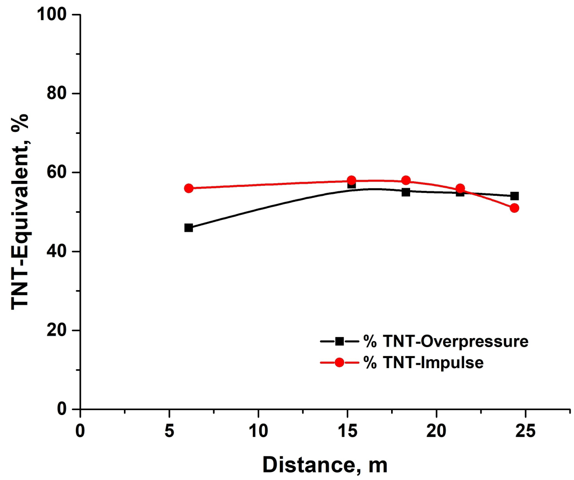

Figure 11. TNT-Equivalent of ANP-3196 from Ref. [37].

Table 14. IM Signature of rocket motors containing NGu/AP/Binder grains.

Formulation	Item	FH	SH	BI	FI	SR
ANP-2874-6	RIM-66B (Standard Missile 2 ER) Aerojet Mk 56 Mod 0 motor	fail	fail	fail	fail	
ANP-3196-1	AGM-45 (Shrike) Aerojet M78 Mod 0 motor	V	IV	IV	IV	
ANP-3196-1	AGM-45 (Shrike) Aerojet M78 Mod 0 motor	V V	III	V V		V pass

Table 15. AP/NGu/Binder Base Bleed Propellants after Ref. [40,41].

Components/Parameters	Unit	10
Nitroguanidine	wt.-%	25
Ammonium perchlorate	wt.-%	55
Styrene/Butadiene copolymer	wt.-%	18
Trioctyl phosphate	wt.-%	2
Density	g cm^{-3}	1.52
T_{ig}	°C	276
Impact-E (BAM)	J	3.4
Friction-F (BAM)	N	160
u at 0.11 MPa	mm s^{-1}	1.11
at 0.89 MPa	mm s^{-1}	3.0
at 1.37 MPa	mm s^{-1}	3.4

2.2.4.2 Base Bleed Applications

As NGu/AP yields a stable burn at atmospheric and even at sub-atmospheric pressures it has been also investigated for base bleed applications (fumers) (Table 15) [40,41].

Investigations extending to much lower pressures and addressing combustion instabilities have been reported in Ref. [42–44] (Table 16).

The Vieille coefficients for the above formulations as a function of service temperature have been determined in Ref. [43] (Table 17).

Table 16. AP/NGu/Binder Propellants [42–44].

Components/Parameters	Unit	11	12	13
Designation		201	200	194
Nitroguanidine	wt.-%	8	10	12
Ammonium perchlorate	wt.-%	66	66	66
Styrene/Butadiene copolymer	wt.-%	22	22	22
Ammonium oxalate	wt.-%	4	2	-
Density	g cm^{-3}			1.614
T_{ig}	°C			
c_{p293}	J g^{-1} K^{-1}			0.743
κ_{295}	W m K^{-1}			0.21
Vieille coefficients $u = a\,p^n$				
u at p > 0.09825 MPa	a			2.765
	n			0.4702
u at 0.005 MPa < p < 0.09825 MPa	a			4.686
	n			0.6976

Table 17. Low pressure Vieille coefficients of NGu/AP propellants [43].

Components/Parameters	Unit	1	12	13
Vieille coefficients $u = a\,p^n$				
Temp 50 °C	a	6.0005	6.7293	4.1993
	n	0.8076	0.8047	0.6371
Temp 25 °C	a	6.3640	11.8358	8.036
	n	0.8762	1.0409	0.87442
Temp −40 °C	a	3.0060	4.2134	10.7689
	n	0.6155	0.6848	1.0059

Table 18. Low pressure Combustion properties of NGu/AP propellant **13** [43].

Thermodynamic Parameters	Unit	at 25.33 kPa	at 101.33 kPa
T_F	K	1777	1779
ρ	kg m^3	0.0341	0.1363
M	g mol^{-1}	19.88	19.89
c_p	J g^{-1} K^{-1}	1.961	1.940
γ	–	1.271	1.275
c	m s^{-1}	1299	1299

The combustion properties of formulation **13** have been calculated at two different pressures (Table 18 and 19).

2.2.4.3 Gas Generator Propellants

Zeuner [45] and later *Lund* [46] have suggested to use a formulation based on NGu and AP in gas generators (Table 20).

NGu stabilizes ammonium perchlorate against thermal decomposition, an effect that appears to be similar to the stabilization of ammonium dinitramide [47].

© 2021 Wiley-VCH GmbH

Table 19. Low pressure Combustion Products of NGu/AP propellant **13** [5].

Combustion Product Mole Fractions	at 25.33 kPa	at 101.33 kPa
CO	0.3005	0.3006
CO_2	0.0331	0.0331
HCl	0.1116	0.1117
H_2	0.3190	0.3191
H_20	0.1298	0.1298
N_2	0.1056	0.1057

Table 20. Composition and Performance of AP/NGu/Binder Propellants from *Lund's* disclosure [46].

Components/Parameters	Unit	14
Designation		EX 10
Nitroguanidine	wt.-%	10
Ammonium perchlorate	wt.-%	46.83
Guanidinium nitrate	wt.-%	23.17
Ammonium nitrate	wt.-%	10.0
Copper(II) oxide	wt.-%	6.0
Carbon	wt.-%	4.0
Density	$g\,cm^{-3}$	1.834
T_f	K	2721
u at 20 MPa	$mm\,s^{-1}$	31.0
Vieille exponent, n	–	0.41

Relatively cool burning gas generator formulations based on GUDN/polyether/BDNPA/F have been studied by *Menke et al.* (Table 21) [48,49] for use with emergency lifting bodies for submarines [50,51]. Table 22 shows the calculated performance parameters for composition **15** and a formulation **15_NGu** in which all FOX-12 is replaced by NGu. While the cold gas composition is very similar for both formulations there is a 4% greater volume with NGu and simultaneously a drop in the combustion chamber temperature by nearly 200 °C which would effect a significant reduced thermal stress to the generator and gas ducts.

Table 22. Calculated performance for composition **1** and **1** modified with NGu in place for FOX-12 [52].

Components/Parameters	Unit	15	15_NGu
Gas composition after expansion to 0.1 MPa			
N_2	Mol/Mol	0.3366	0.3649
CO	Mol/Mol	0.1466	0.1314
H_2	Mol/Mol	0.2575	0.2839
H_2O	Mol/Mol	0.1012	0.0934
CO_2	Mol/Mol	0.1356	0.1001
CH_4	Mol/Mol	0.0224	0.0262
T_{ad} at 7 MPa	°C	1616	1429
Gas yield at 0.1 MPa and expansion temperature	$L\,kg^{-1}$	3311	3443
Exhaust temperature after expansion (70:1)	°C	623	626

3 Gun Propellants

Very early after the first synthesis and characterization of nitroguanidine by *Thiele* (1892) based on its basicity *Flemming* (1898) suggested to use NGu as a stabilizer for nitrocellulose [53]. *Vieille* (1900) in his seminal study on the erosion of gun propellants appears to have been the first to study the influence of the cool burning NGu on gun propellants and explicitly refers to *Flemming's* suggestion to use NGu [54]. One of the first patents teaching the use of NGu in gun propellants was filed by *Abelli* in 1905 [55]. An extensive account of the development and use of NGu in flashless gun propellants in Europe until the end of WWII was prepared by *Pring* in 1948 and later declassified [56].

3.1 Formulations

A key step in the development of gun propellants was the invention of the German Gudol powder (RP-39) in the

Table 21. Composition and Performance FOX-12 based cold gas generators [48,49].

Components/Parameters	Unit	15	16	17	18	19
FOX-12	wt.-%	70	70	70	75	35.6
FOX-7	wt.-%					34.4
GAP	wt.-%	11.2			10	
Polyester	wt.-%		8.4			
Polyether	wt.-%			8.4		14
BDNPA/F	wt.-%	13.4	19.6	19.6		14
Triacetin	wt.-%	3.4			13	
CeO_2	wt.-%	1	1	1	1	1
Y_2O_3	wt.-%	1	1	1	1	1
ρ	$g\,cm^{-3}$	1.625	1.619	1.604	1.607	1.605
T_f	°C	1387	1371	1253	1048	1162
Burning rate at 10 MPa	$mm\,s^{-1}$	6.7	6.5	5.8	3.8	4.9
Gas yield at STP	$L\,kg^{-1}$	1061	1054	1093	1072	1121
Exhaust temperature after expansion (70:1)	°C	327	327	267	188	224

 © 2021 Wiley-VCH GmbH

Table 23. Composition of experimental and in-service gun propellants containing NGu.

Component	Unit	M15	M30	HUG	MTLS	HUX	MRCA
	Alternative Designations	N6060, NQ	N6540, IN5340,		R5730	H1707	Q5560
NGu	wt.-%	54.54	47.54	30	32.4	8.6	5.5
NC	wt.-%	19.94	27.9	24	33	52	74
(N-content)	wt.-%	(13.15)	(12.6)		(12.5)		(13.1)
NGl	wt.-%	18.94	22.42	16			
DEGN	wt.-%	–			22.1		18
TEGDN	wt.-%	–				26	
RDX	wt.-%	–		30	7.5	10.7	
Na_3AlF_6	wt.-%	0.3	0.3				
K_2SO_4	wt.-%				0.31	1.0	1.0
Ethylcentralite	wt.-%	5.98	1.49				
Ethylphenylurethane	wt.-%				0.73	1.0	
Diphenylurethane	wt.-%				0.70		
Akardite II	wt.-%				0.74		1
Graphite	wt.-%		0.3		0.1		
Ethanol	wt.-%	0.3	0.3				
Water	wt.-%				0.61		0.5

1930s. This was achieved in a joint effort directed by *von Gallwitz*,[1] *Poppenberg*[2] and WASAG [57,58a].

Gudol propellant, RP-39 often referred to as "Gudol" only

- NC (12.2 % N) 35.49 wt.-%
- NGu 40.00 wt.-%
- DEGDN 21.76 wt.-%
- Akardite 0.50 wt.-%
- Ethylphenylurethane 0.70 wt.-%
- Diphenylurethane 0.70 wt.-%
- K_2SO_4 0.50 wt.-%
- Graphite 0.35 wt.-%

RP-39 propellant contains nitrocellulose as an energetic base and binder, nitroguanidine, and diethylene glycol dinitrate (DEGDN). The latter, which was a replacement for nitroglycerine, as glycerine was at short supply in Germany due to its provenience from natural fat [58b]. Both NGu and DEGDN afford low combustion temperature and hence yield low erosion and reduced muzzle flash.

Standard NGu-based propellants developed after the war in the US and UK (**M15**, **NQ**, and **M30**) however, continue to use nitroglycerine as blasting oil and gelling agent for NC.

In post-war Germany on the contrary, several propellants resembling the original Gudol propellant were produced again. These include **P5450**, which is practically identical to **RP-39**; **P5440**, which has a different NC/NGu// DEGDN ratio and is also modified with additional KNO_3 and finally **P5430**, which has a slightly higher DEGDN-content [59,60]. In the 1990s *Proksch-Jeck* further modified **P5450** to meet modern requirements for use in 155 mm howitzer by replacement of 7 wt-% NGu with RDX to give **R5430** propellant which is also known as **MTLS** propellant [61,62].

While the Gudol propellants were initially developed for use in large-caliber weapons, changing the ratio of ingredients also allows the use of **Gudol** powders in medium caliber weapons. In the 1970s, in the course of the development of the Mauser BK 27 mm automatic cannon for the Tornado aircraft, *Brachert et al.* developed a Gudol propellant with low NGu content (5 wt.-%) [63,64].

The French **HUX** propellant finally is related to **MRCA** but uses an even less energetic plasticizer TEGDN [65,66] which was also initially suggested by *von Gallwitz* as a moderately energetic base and plasticizer for NC [57]. Table 23 shows state-of-the-art gun propellants containing nitroguanidine.

A series of experimental formulations containing NGu developed by Eurenco [65], Fraunhofer ICT [67–69], and French-German ISL [70] is given in Table 24.

Braithwaite et al. have investigated the influence of NGu on ETPE-based propellants (Hytrel™ or BAMO/AMMO) together with either CL-20 or RDX [71–73] (Table 25 and 26). *Penney et al.* have invented insensitive formulations (**503–521**) containing NGu as given in Table 27 [74].

Table 28 finally describes both **M30** and **MRCA** propellants modified with LTC plasticizer DNDA-5,7 as reported by *Mueller* [75], a NILE formulation containing NGu for comparative purposes, and two experimental semi-nitramine propellants invented at Picatinny Arsenal [76–79].

With the advent of FOX-12, corresponding gun propellant formulations have been first described by *Dahlberg et al.* [80]. He modified the insensitive propellant **M43** (RDX, CAB, BDNPF–A/NC)(Table 29) by successive replacement of RDX with FOX-12 to give **NL-100** propellant. A later for-

[1] *Major general Dr. Ing. Uto Gallwitz*, (1892-1943) Head of propellant development at Heereswaffenamt (HWA), Berlin.

[2] *Prof. Dr. phil. Otto Poppenberg* (1876–1956) Explosive chemist and ballistics expert, director of Institut für Sprengstoffchemie (engl: Institute for the chemistry of explosives) at TH Berlin-Charlottenburg.

© 2021 Wiley-VCH GmbH

Table 24. Experimental gun propellants containing NGu (I) [65,67,69,70].

Component	Unit	KHP 158	KHP 167	KHP 168	KHP 265	KHP 290	KHP 300	KHP 301	KHP 230	NENA-NQ20	NENA-NQ40
Density	$g\,cm^{-3}$									1.627	1.667
RDX	wt.-%	59	77.2	42.5	75	79.2	79.0	61.0	79.1		
NGu	wt.-%	26	8	42.5	10	10.0	8.0	26.0	10	20	40
NC-13.1	wt.-%									39.56	29.67
DINA	wt.-%									27.76	20.82
NGl	wt.-%										
Me-NENA	wt.-%									11.88	8.91
GAP	wt.-%						13.0	13.0			
PB	wt.-%	11	10.8	11.0	11	10.8			10.9		
KNO_3	wt.-%	4	4	4.0	4						
EC	wt.-%									0.8	0.6

Table 25. Experimental gun propellants containing NGu (II) [71–73].

Designation	Unit	O1	O1a	O2	O3	O3-1	O3-2	O3-3	O4
Density	$g\,cm^{-3}$	1.705		1.684	1.618	1.604	1.598	1.585	1.627
NGu	wt.-%	24	20	32	24	24*	18*	12*	30
RDX	wt.-%				52	52	56.5	60	48
CL-20	wt.-%	52	56	44					
BAMO	wt.-%	6	6	6	6	8.4	8.925	9.8	5.5
AMMO	wt.-%	18	18	18	18	15.6	16.575	18.2	16.5

*) with HBNQ.

Table 26. Experimental gun propellants containing NGu (III) [71–73].

Designation	Unit	H1	H2	H2M	H3	H4
Density	$g\,cm^{-3}$	1.65	1.65	1.64	1.67	1.68
NGu	wt.-%	32	20	19.2	32	26.67
RDX	wt.-%	49	60	57.7	54	60
BDNPA/F	wt.-%	5	6.67	10.3		
Hytrel™ *	wt.-%	14	13.3	12.8	14	13.33

*) Thermoplastic polyester.

mulation is given in Table 29. Sometime after that *Walsh* and *Knott* followed the same concept [81] but then decided to adopt an all non-energetic binder to further reduce the heat of explosion, temperature, and consequently the degree of erosion [82]. This however also leads to the lowest performance of all gun propellants discussed in the context of this review. Yet another propellant formulation containing FOX-12 and based on **M39** has been formulated by *Mason* [83].

Table 27. Experimental gun propellants containing NGu (IV) [74].

Designation	Unit	503	516	519	521
NGu	wt.-%	18.5	10	18.5	10
HMX	wt.-%		70	56	
RDX	wt.-%	56			70
NC	wt.-%	8.5		8.5	
Bu-Nena	wt.-%	6	5	6	5
DOA	wt.-%	3	4	3	4
Carbamite	wt.-%	1		1	
EVA	wt.-%	7	11	7	11
Akardite II	wt.-%	0.7			
Dioctylphthalate	wt.-%	1.0		8.0	5.0
Centralite I	wt.-%	1.0	0.4		1.5

Some propellants containing neither NGu nor GUDN are given for reference and comparison in Table 30.

3.2 Ballistic Performance

The ballistic performance of a gun propellant can be calculated with reasonable accuracy with thermochemical codes [85] or other numerical methods [86]. For the present review, the calculations were performed with *Cheetah 2.0* [52] at a loading density of $\Delta = 0.2\ g\,cm^{-3}$ using BKWC library

© 2021 Wiley-VCH GmbH

Table 28. Experimental modifications of NGu based gun propellants.

Component	Unit	M30-EPX	MRCA-EPX	NILE-NGu*	NT	HFP
Alternative Names					PPL-A-6396	PPL-A-6372
RDX	wt.-%			40	34.5	36.5
NGu	wt.-%	47.5	6.2	32	7	5
NC-13.1	wt.-%	27.0	69.8		28.5 (12.6)	29.3 (12.6)
Ngl	wt.-%				20.5	22.7
DNDA-5,7	wt.-%	24	22.3			
CAB	wt.-%			14.4		
ATEC	wt.-%			7.2		
HPC	wt.-%			5.3		
Vestenamer	wt.-%			0.7		
Akardite II	wt.-%		0.7			
Dioctylphthalate	wt.-%		1.0		8.0	5.0
Centralite I	wt.-%	1.0		0.4		1.5
Na_3AlF_6	wt.-%	0.5			1.5	

*) NILE with the same weight fraction of NGu instead of FOX-12.

Table 29. Experimental and state of the art gun propellants containing FOX-12 [80–83].

Component	Unit	NL-100	NILE	HFR-001	EX-99-10	EX-99-20
RDX	wt.-%	16	40	40	66	56
FOX-12	wt.-%	60	32	30	10	20
TEGDN	wt.-%			13.5		
ATEC	wt.-%		7.2			
TGDE	wt.-%			6.6		
CAB	wt.-%		14.4		12	12
Polycaprolactone	wt.-%			7.9		
BDNPA/F	wt.-%				7.6	7.6
Curing agents	wt.-%			2		
HPC	wt.-%		5.3			
Vestenamer TM 6213	wt.-%		0.7			
Centralite I	wt.-%	0.5	0.4		0.4	0.4
Graphite	wt.-%				0.1	0.1
NC	wt.-%	11.75			4	4
Bu-NENA	wt.-%	11.75				

and with activated Blake Code compatibility to enable comparison with other reference publications [87]. Table 31 lists the calculated and in some cases experimentally reported performance, determined as a *force* for the reference gun propellants. Figure 12 displays the force versus temperature of all the propellants considered in this review with colored coding to reveal the different compositional types. The reference propellants are indicated by filled black circles.

Table 32 displays the performance of NGu-containing propellants with NC as binder and either DEGDN or NGl content which are depicted as magenta filled squares in Figure 12. Both *Vanderhoff* [88] and *Langlotz* [89] have determined the burning rate though in different pressure regimes as is depicted in Figure 13. *De Luca et al* have studied the influence of particle size of NGu on burning rate of **M30** [90]. Their study confirms the intuitive perception that small particles due to their inherent greater surface area burn quicker and hence closer to the surface of a grain thereby improving heat feedback and speeding up overall burning rate which is depicted in Figure 14. The temporal enhancement of burning rate of **M30** grains due to plasma ignition (ETC), ($u = 11.441p^{0.456}$) has been investigated by *Birk et al* in Ref. [91]. The influence of different types of nitrocellulose on both **M15** and **M30** type propellant has been studied in Ref. [92]. The influence of strand diameter on pressure rise and burning rate of M30 has been studied in Ref. [93]. Ballistic properties of a modified **M30** propellant obtained from TSE are presented in Ref. [94].

NGu-NC-nitrate ester (NE) formulations with additional RDX are described below in Table 33 and are given as filled red stars in Figure 12. The coordinates in the T/*f*—diagram correlate with the type of nitrate ester: That is, NGl-based propellants yield both higher temperature and force whereas both DEGDN and TEGDN yield lower values. Figure 15 displays the burning rate of **HUG** which reveals an increasing pressure dependence with increasing pressure.

 © 2021 Wiley-VCH GmbH

Table 30. Reference Propellants [84a].

Component	Unit	*A5020*	*GB-Pa-125*	M39	M43
Type		Single base	Double base	LOVA	LOVA
Alternative Designation					EX99
RDX	wt.-%			76	76
NC-13.1	wt.-%	95	70	6.3	4
Ngl	wt.-%		30		
CAB	wt.-%			11	12
ATEC	wt.-%			6	
Diphenylamine	wt.-%	0.8			
BDNPA/Fr	wt.-%				8
Dibutylphthalate	wt.-%	1.3			
Dioctylphthalate	wt.-%	1.3			
Centralite I	wt.-%	1.5	+1.5 (additive)	0.4	0.4

Table 31. Measured and calculated properties of state-of-the-art gun propellants containing NGu or FOX-12 and equilibrium composition of gases based on loading density of $\Delta = 0.2\ g\,cm^{-3}$ [52].

Parameter	Unit	*A5020*	*GB-Pa*	*M39*	*M43*
Temperature	K	2873	3778	2830	3180
Covolume	$g\,cm^{-3}$	1.045	0.95	1.145	1.115
Pressure	MPa	255.8	287.4	288.0	311.4
Force calculated	$J\,g^{-1}$	1011.81	1164	1110	1210
Force measured at Δ	$J\,g^{-1}$				1181 Δ?
Molecular weight	$g\,mol^{-1}$	23.611	26.981	21.192	21.855
Gamma	–	1.247	1.211	1.264	1.253
Equilibrium composition after *Cheetah 2.0*					
CO	Mol/Mol	0.4694	0.3073	0.3869	0.3658
N_2	Mol/Mol	0.1068	0.1403	0.2229	0.2384
H_2	Mol/Mol	0.1435	0.0468	0.2284	0.1946
H_2O	Mol/Mol	0,1958	0.2812	0.1290	0.1602
CO_2	Mol/Mol	0.0821	0.2021	0.0281	0.0358
NH_3	Mol/Mol			0.0016	0.0011
CH_4	Mol/Mol				

Table 34 shows the performance of experimental formulations developed at Fraunhofer ICT based on both HTPB and GAP. In Figure 12 those HTPB based formulations are violet filled hexagons whereas the GAP based formulations are light blue filled squares. Both **KHP-168** (HTPB) and **KHP-300** (GAP) yield the top-notch force at their corresponding temperature being approximately 20% more powerful, than comparable NC-NGu-NE formulations. Figure 15 depicts the burning rate of two KHP propellants. **KHP-290** with increased RDX content over **KHP-265** shows a significantly higher pressure exponent than the former. The NENA modified NC- based formulations (orange triangles in Figure 12) show performance pretty much in line with NGU-NC-RDX-NE group and are tentatively weaker than the latter. The burning rate at 100 MPa is shown in Table 35 and depicted also in Figure 15 as open circle and cross.

The propellants with BAMO-AMMO binder with RDX (grey triangles) or CL-20 (light blue pentagons) are generally more powerful than NC based ones (Table 36). Propellant **O1a** with 56 wt-% CL-20 is as powerful as the double base reference propellant **GB-Pa** but is burning nearly 900 K cooler which will have reduced erosion. Propellant **O3-3** with 60 wt-% RDX is as powerful as M43 and burns about 300 K cooler.

The combustion properties for **O3** have been determined in the temperature range between −32 and +49 °C (Table 37) [73]. However, as is evident from tables 37 and 38, the coefficients found in either table for **O3** do not match as they stem from four different facilities involved in this study and highlight the need for regular round-robin tests. The burning rates of **O3-1–O3-3** using HBNQ are given in Table 39 and displayed in Figure 16.

NGu-RDX-Propellants with the non-energetic Hytrel™-binder (light green triangles) yield lower performance than **O3-n** formulations (Table 40). Vieille's law in the pressure

© 2021 Wiley-VCH GmbH

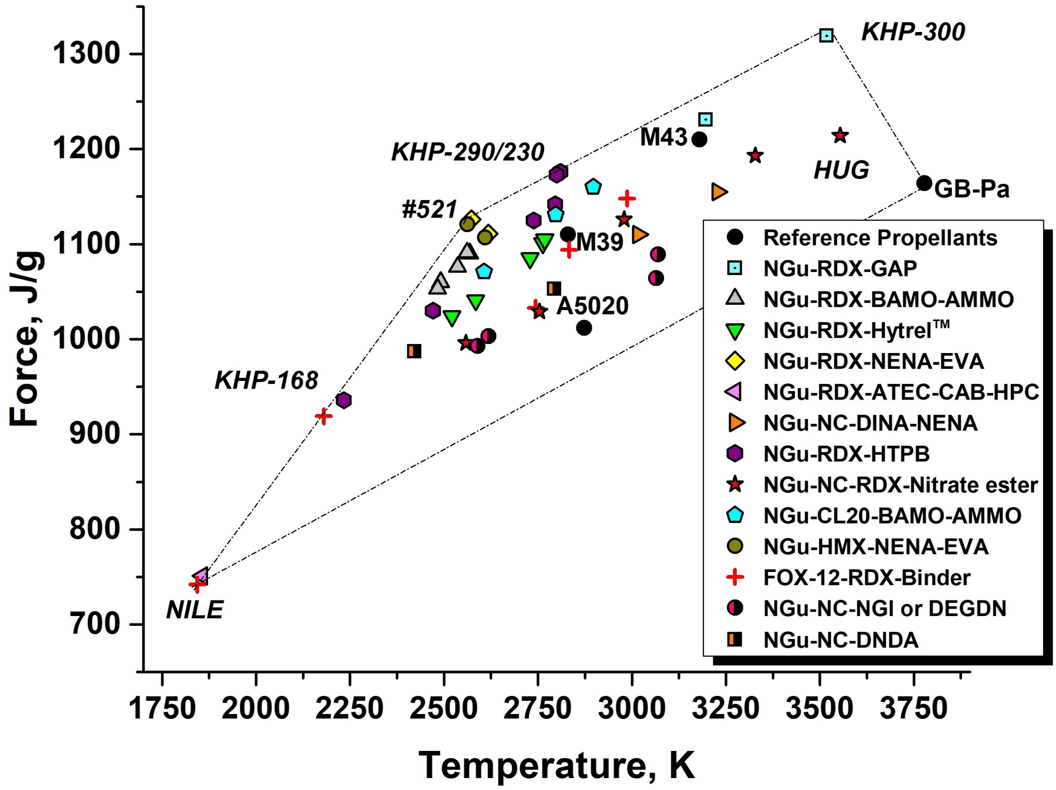

Figure 12. T/Force diagram of gun propellants.

Table 32. Measured and calculated properties of gun propellants containing NGu equilibrium composition of gases based on loading density of $\Delta = 0.2\ g\,cm^{-3}$ [52].

Parameter	Unit	M15	M30	MRCA	Gudol RP-39
Temperature	K	2619	3070	3065	2589
Covolume	$cm^3 g^{-1}$	1.110	1.038	1.011	1.096
Pressure	MPa	257.8	274.9	266.7	254.4
Pressure measured at Δ	MPa			178.9 at $\Delta = 0.15$	
Heat of explosion	$J g^{-1}$	3175	4045	3997 [95]	2866
Force calculated	$J g^{-1}$	1002.7	1089	1064	993
Force measured at Δ	$J g^{-1}$				930 (Δ?)
Molecular weight	$g\,mol^{-1}$	21.724	23.445	23.958	21.678
Gamma	–	1.261	1.240	1.236	1.259
Equilibrium composition after *Cheetah 2.0*					
CO	Mol/Mol	0.3040	0.2729	0.3921	0.3368
N_2	Mol/Mol	0.2797	0.2801	0.1311	0.2255
H_2	Mol/Mol	0.1966	0.1206	0.1195	0.1970
H_2O	Mol/Mol	0.1773	0.2521	0.2531	0.1921
CO_2	Mol/Mol	0.0378	0.0694	0.1014	0.0458
NH_3	Mol/Mol	0.0015	0.0005	0	0.0014
CH_4	Mol/Mol	0	0	0	0

range between 50–300 MPa for **H2M** propellant reads $u = 0.224\ p^{1.164}$ [73].

The EVA-BuNENA formulations containing either HMX (olive circles) or RDX (yellow diamonds) yield the highest

© 2021 Wiley-VCH GmbH

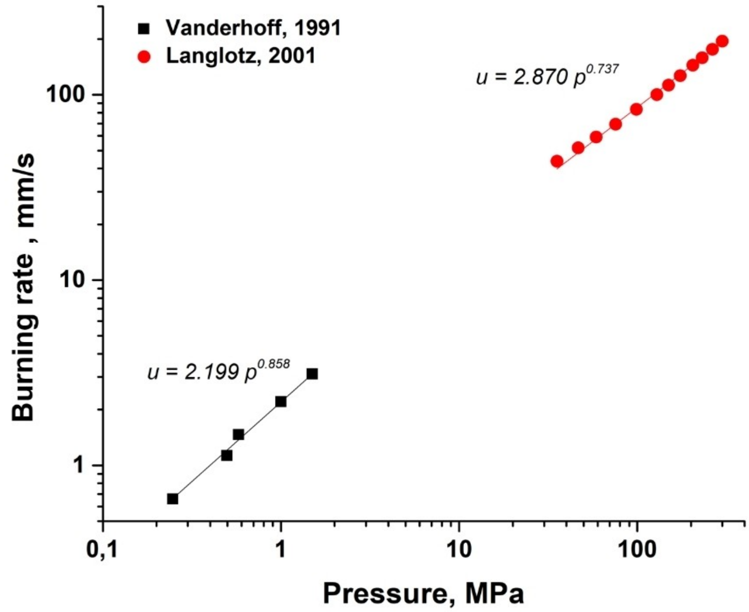

Figure 13. Burning rate of M30 propellant.

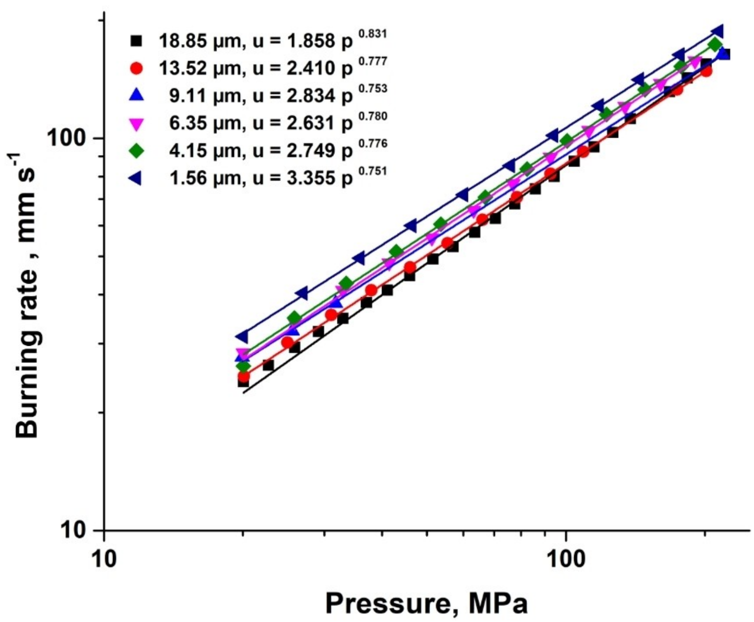

Figure 14. Burning rate of M30 propellant with different NGu particle sizes [90].

calculated performance at their corresponding temperature of all considered propellants in this review (Table 41).

Replacing nitroglycerine in either **M30** or **MRCA** with DNDA-5,6 yields both a big drop in combustion temperature and a drop in force by 6 and 2%. In Figure 12 those two formulations are the orange-black striped squares (Table 42).

All FOX-12 containing propellants (Table 43) are indicated with red crosses in Figure 12. *Dahlberg* first reported about an experimental **NL1**-propellant containing 60% GUDN in 2005 (Table 44). He found a low-pressure exponent up to 40 MPa and a high value for n ~ 0.957 at pressures beyond 40 MPa [80].

Later *Dahlberg* reported a modification of the propellant with a higher percentage of RDX which furnished a more uniform combustion behaviour still with high overall pressure exponent (n ~ 0.931) [99]. The experimental burning rate of FOX-12 based propellants **NL-100** and **NILE** [82] are

 © 2021 Wiley-VCH GmbH

Table 33. Measured and calculated properties of gun propellants containing NGu equilibrium composition of gases based on loading density of $\Delta = 0.2\ g\,cm^{-3}$ [52].

Parameter	Unit	HUG	MTLS	HUX	NT	HFP
Temperature	K	3554	2558	2754	2979	3328
Covolume	cm^3g^{-1}	1.019	1.117	1.070	1.100	1.057
Pressure	MPa	304.9	256.6	261.9	288.8	302.6
Heat of explosion	$J\,g^{-1}$	1214	3680			
Force calculated	g^{-1}	1222	996.3	1029.05	1126	1193
Force measured at Δ	$J\,g^{-1}$			1065 (Δ?)		
Molecular weight	$g\,mol^{-1}$	24.354	21.351	22.251	21.992	23.189
Gamma	–	1.229	1.264	1.252	1.254	1.241
Equilibrium composition after *Cheetah 2.0*						
CO	Mol/Mol	0.2566	0.3623	0.4059	0.3981	0.3713
N_2	Mol/Mol	0.2914	0.2132	0.1491	0.1904	0.2026
H_2	Mol/Mol	0.0870	0.2160	0.1814	0.1911	0.1403
H_2O	Mol/Mol	0.2669	0.1650	0.1995	0.1722	0.2144
CO_2	Mol/Mol	0.0881	0.0390	0.0590	0.0445	0.0657
NH_3	Mol/Mol		0.0017	0.0009	0.0010	0,0001
CH_4	Mol/Mol		0	0		

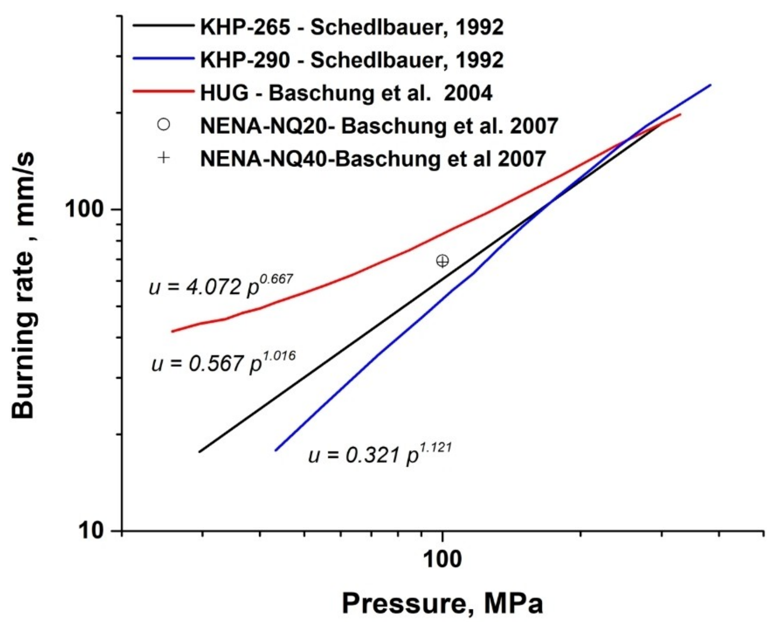

Figure 15. Burning rate of HUG, KHP-265, and KHP-290.

depicted in Figure 17 together with Vieille's law for the individual propellants. Mason determined the burning rate for **HFR-001** which is also depicted in Figure 17.

The dotted quadrangle shown in Figure 12 shows the range of properties available with NGu based propellants if modifications with binders and auxiliary energetic fillers are considered. Most importantly many formulations yield force values by on average 50–70 J/g higher than with any of the conventional NC-NE formulations. This higher performance comes with a drop in temperature which, based on the important relationship between explosion temperature and erosion $E \sim T^7$ [84b], has a significant impact on gun barrel lifetime.

3.3 Combustion Spectroscopy and Signature

UV-VIS spectroscopic investigations of M 30-gun propellant deflagration flames under 1 MPa nitrogen pressure indicate significant levels of NH (43 ppm at 1 MPa) which is in line

© 2021 Wiley-VCH GmbH

Table 34. Reported performance data of *experimental* gun propellants containing NGu [96–98].

Component	Unit	KHP 158	KHP 167	KHP 168	KHP 265	KHP 290	KHP 300	KHP 301	KHP 230	NENA-NQ20	NENA-NQ40
Oxygen balance	wt.-%			-41.2			-36.1	-37.7			
Temperature	K	2471	2796	2234	2739	2810	3518	3196	2800	3228	3017
Covolume	cm^3g^{-1}	1.209	1.187	1.219	1.192	1.214	1.113	1.136	1.215	1.041	1.065
Pressure	MPa	271.8	299.5	247.6	295.4	310.6	339.3	318.6	310.0	291.7	282.0
Heat of explosion	$J g^{-1}$					3660	4354				
Force calculated	$J g^{-1}$	1030	1142	936	1125	1176	1319	1231	1173	1155	1110
Force measured	$J g^{-1}$	916	948					1128			
Molecular weight	$g\ mol^{-1}$	19.945	20.357	19.846	20.25	19.865	22.187	21.588	19.838	23.240	22.604
Gamma		1.278	1.271	1.280	1.273	1.273	1.249	1.255	1.215	1.238	1.245
Equilibrium Composition after *Cheetah 2.0*											
CO	Mol/Mol	0.3504	0.3724	0.3269	0.3713	0.3727	0.3079	0.2899	0.3733	0.3338	0.2953
N_2	Mol/Mol	0.2591	0.2449	0.2761	0.2451	0.2474	0.3134	0.3270	0.2468	0.2125	0.2634
H_2	Mol/Mol	0.2960	0.2785	0.2968	0.2835	0.2916	0.1761	0.2023	0.2928	0.1318	0.1517
H_2O	Mol/Mol	0.0626	0.0750	0.0587	0.0709	0.0675	0.1624	0.1499	0.0661	0.2445	0.2311
CO_2	Mol/Mol	0.0108	0.0131	0.0106	0.0123	0.0112	0.0318	0.0254	0.0109	0.0729	0.0955
NH_3	Mol/Mol	0.0034	0.0024	0.0043	0.0026	0.0027			0.0027	0.3338	0.2953
CH_4	Mol/Mol	0.0054	0.0013	0.0146	0.0018	0,0018			0,0019		

Table 35. Experimental density and burning rate of NENA-NQ propellants [71].

Propellant	Density (g/cm^3)	*u* at 100 MPa (mm/s)
NENA-NQ20	1.627	69.4
NENA-NQ40	1.667	68.7

with the predicted concentrations for the parent molecule NH_3 (Table 43) [85,88,100,101]. *Anderson* has modelled the combustion of M30 propellant. He found that the transient species NH, NH_2, and NH_3 – uniquely formed in NGu based propellants – have a key role in that they react swiftly with NO. While NO forms in large amounts too with single and double base propellants, the absence of NH_x yields a distinct dark zone with the latter propellants not found with either pure NGu or the propellants based on it [102]. Due to the absence of the dark zone, the heat feedback to the burning surface is improved and consequently the burning rate is altered.

Table 36. Calculated properties of BAMO-AMMO based propellants with loading density of $\Delta = 0.2\ g\,cm^{-3}$ [52].

Parameter	Unit	O1	O1a	O2	O3	O3-1	O3-2	O3-3	O4
Temperature	K	2797	2897	2607	2491	2536	2568	2561	2483
Covolume	cm^3g^{-1}	1.212	1.205	1.226	1.241	1.238	1.241	1.248	1.235
Pressure	MPa	298.5	305	283.9	282.1	285.9	290.1	290.8	279.7
Force calculated	$J g^{-1}$	1131	1160	1071	1060	1076	1090	1091	1053
Molecular weight	$g mol^{-1}$	20.570	20.763	20.234	19.534	19.603	19.578	19.515	19.601
Gamma	–	1.276	1.274	1.279	1.280	1.279	1.279	1.279	1.279
Equilibrium composition after *Cheetah 2.0*									
CO	Mol/Mol	0.3604	0.3677	0.3458	0.3342	0.3327	0.3426	0.3534	0.3232
N_2	Mol/Mol	0.3034	0.3019	0.3068	0.2852	0.2894	0.2819	0.2736	0.2934
H_2	Mol/Mol	0.2705	0.2627	0.2833	0.3067	0.3043	0.3066	0.3105	0.3022
H_2O	Mol/Mol	0.0469	0.0492	0.0432	0.0489	0.0507	0.0450	0.0353	0.0575
CO_2	Mol/Mol	0.0082	0.0087	0.0073	0.0077	0.0079	0.0071	0.0057	0.0089
NH_3	Mol/Mol	0.0026	0.0023	0.0031	0.0039	0.0037	0.0036	0.0037	0.0036
CH_4	Mol/Mol	0.0019	0.0013	0.0041	0.0073	0.0058	0.0062	0.0088	0.0059

© 2021 Wiley-VCH GmbH

Table 37. Vieille's coefficients for combustion of propellant formulation **O3** in the pressure regime between 96.5 MPa and 355 MPa at different temperatures [73].

Facility	Temperature °C	a	n
ARDEC	-32	0.4549	0.985
Thiokol	21	1.0362	0.929
ARDEC	21	0.5781	0.971
ARDEC	49	0.5387	0.980

Table 38. Vieille's coefficients for combustion of propellant formulation **O1** and **O3** at 96.5 MPa at different temperatures [73].

Formulation	Burning rate at 275.8 MPa mm s^{-1}			Pressure exponent at 275 MPa		
Temperature (°C)	−32	20	50	−32	20	50
O1	170.43	178.05	187.71	0.98	1.00	1.00
O3	101.09	105.41	111.00	0.88	0.87	0.89

According to Ref. [103], potassium hydrogen carbonate, $KHCO_3$, is the most effective additive to suppress a muzzle flash upon firing M30 propellant.

3.4 Physical Properties of Propellants

The introduction of fibrous nitroguanidine into propellants yields considerable anisotropy of physical properties as is evident from Figure 18 which depicts the thermal conductivity and diffusivity in a M30 propellant grain. The specific heat of M30 as a function of temperature is depicted in Figure 19 [104].

The mechanical properties of the TPE based propellants **O1**, **O3**, and **H2** are compared to standard **M30** in Table 45. **M30** with the highest amount of fibrous NGu exhibits the greatest mechanical strength followed by **O3** and **O2. Now H2-HBNQ** utilizing non fibrous but brick shaped NGu and the lowest NGu content on top shows the lowest mechanical performance.

Table 39. Burning rates of **O3-1, O3-2 O3-3** at various pressures [73].

	Measured Density g cm^{-3}	Temperature °C	Burning rate at pressure (MPa) mm s^{-1}			Pressure exponent
			137.9	206.8	241.3	
O3-1	1.602	23.3	64.516	94.361	107.873	0.918
O3-2	1.595	22.7	67.132	97.993	113.081	0.932
O3-3	1.582	22.6	67.335	98.425	112.979	0.925

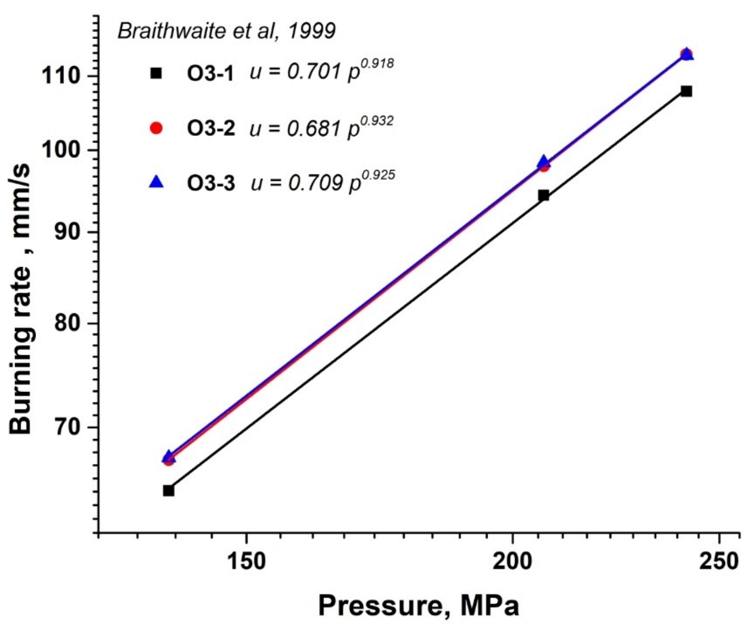

Figure 16. Burning rate of BAMO-AMMO based propellants.

© 2021 Wiley-VCH GmbH

Table 40. Ballistic properties of **H**-gun propellants at a loading density of $\Delta = 0.2\ g\,cm^{-3}$ [52].

Parameter	Unit	H1	H2	H2 M	H3	H4
Temperature	K	2521	2763	2768	2584	2729
Covolume	$cm^3\ g^{-1}$	1.177	1.160	1.160	1.170	1.159
Pressure	MPa	267.8	286.9	287.8	271.7	282.5
Force calculated	$J\,g^{-1}$	1024	1101	1105	1041	1085
Molecular weight	$g\ mol^{-1}$	20.48	20.86	20.82	20.66	20.91
Gamma	–	1.273	1.266	1.266	1.271	1.267
Equilibrium composition after *Cheetah 2.0*						
CO	Mol/Mol	0.3380	0.3510	0.3549	0.3304	0.3331
N_2	Mol/Mol	0.2659	0.2563	0.2509	0.2757	0.2750
H_2	Mol/Mol	0.2577	0.2407	0.2420	0.2495	0.2376
H_2O	Mol/Mol	0.1114	0.1233	0.1236	0.1169	0.1260
CO_2	Mol/Mol	0.0209	0.0236	0.0238	0.0216	0.0235
NH_3	Mol/Mol	0.0026	0.0020	0.0020	0.0024	0.0020
CH_4	Mol/Mol	0.0015	0.0001	0.0001	0.0010	0.0001

Table 41. Calculated ballistic properties of EVA-based-gun propellants containing NGu at a loading density of $\Delta = 0.2\ g\,cm^{-3}$ [52].

Parameter	Unit	503	516	519	521
Temperature	K	2619	2562	2610	2573
Covolume	$cm^3 g^{-1}$	1.211	1.245	1.211	1.245
Pressure	MPa	293.1	298.6	292.0	300
Heat of explosion	$J\,g^{-1}$				
Force calculated	$J\,g^{-1}$	1111	1121	1107	1126
Molecular weight	$g\,mol^{-1}$	19.605	18.997	19.608	18.989
Gamma	–	1.274	1.277	1.274	1.277
Equilibrium composition after *Cheetah 2.0*					
CO	Mol/Mol	0.3627	0.3742	0.3627	0.3743
N_2	Mol/Mol	0.2321	0.2187	0.2322	0.2186
H_2	Mol/Mol	0.2966	0.3256	0.2965	0.3261
H_2O	Mol/Mol	0.0848	0.0552	0.0848	0.0551
CO_2	Mol/Mol	0.0142	0.0089	0.0143	0.0088
NH_3	Mol/Mol	0.0030	0.0037	0.0031	0.0037
CH_4	Mol/Mol	0.0026	0.0073	0.0027	0.0071

3.5 Erosivity

While the performance of propellant is unambiguously described by its force and other thermodynamic figures of merit, which can be predicted with good accuracy, it lacks such unambiguous parameters when it comes to the assessment of the erosive nature of hot propellant gases.[3] However, *Stein* found that the explosion temperature plays a major role on erosion with a relationship of the kind $E \sim T^7$ [84b].

Typically, the erosivity of propellants is measured in a so-called *erosion bomb* originally invented by *Vieille* [54]. This is a ballistic bomb fitted with a burst disk and nozzle. Upon firing a propellant charge the burst disk ruptures at a predetermined pressure and the combustion products flow out through the nozzle causing erosion to it. Both rupture pressure and mass loss of the nozzle are taken into account in assessing the erosivity. Similar test set ups use instrumented guns with burst disks. A series of studies has been conducted in a 37 mm Blow Out Gun as depicted in Figure 20. The results for **M30** and other NGu-containing propellants are given in Table 46.

In a French study, the erosion of conventional single-, double-, nitramine, and triple base propellants have been compared in Table 47 [65]. In a later study, *Baschung et al.* found qualitative proof that **HUG** propellant is however more erosive than initially determined [108].

[3] Ref. [106] describes small arms (4.6 – 12.7 mm) tests to determine the degradation of gun barrels, that is the combination of erosion and wear, caused by firing shells. Ref. [107] describes such test procedures for tank and artillery cannons.

 © 2021 Wiley-VCH GmbH

Table 42. properties of DNDA-modified gun propellants [52].

Parameter	Unit	M30-EPX	MRCA-EPX
Oxygen balance	wt.-%	−44.36	−44.51
Temperature	K	2422	2793
Covolume	cm^3g^{-1}	1.158	1.088
Pressure	MPa	256.8	269.1
Force calculated	$J g^{-1}$	986.6	1052.9
Molecular weight	$g mol^{-1}$	20.415	22.063
Gamma	–	1.271	1.255
Equilibrium composition after *Cheetah 2.0*			
CO	Mol/Mol	0.3059	0.4261
N_2	Mol/Mol	0.2678	0.1557
H_2	Mol/Mol	0.2512	0.1898
H_2O	Mol/Mol	0.1436	0.1826
CO_2	Mol/Mol	0.0260	0.0523
NH_3	Mol/Mol	0.0027	

Zimmermann et al. compared the erosion of different conventional and LOVA propellants [96] by using a 20 mm gun with a tube insert to determine erosion (Table 48).

Hordijk et al. have investigated the erosivity of various single, double, triple-base, and LOVA formulations [110,111]. They found that **MTLS** propellant shows a significantly lower wear rate (0.002 m/s) on gun barrels than RDX/CAB based LOVA-propellants of similar force ($f\sim$ 1000 $J g^{-1}$) (0.02–0.1 m/s).

Dahlberg did erosion bomb measurements on **NL-100** and **M30** reference propellant (Table 49), [109]. *Lawton*'s erosivity, A(m/s), (see equation (2) and (3)) [112] does not even remotely fit any of the observed experimental erosivities (Figure 21–25) thus questioning the validity of *Lawton's* equation and the general concept behind.

Table 44. Vieille's law coefficients of experimental **NL-1** propellant based on 60 wt.-% GUDN [80].

Pressure range	a	n
40–100 MPa	2.50	0.598
100–300 MPa	0.443	0.957

$$A = 114\ e^{0.0207\ x}, \qquad (2)$$

With

$$x = [CO]\text{-}3.3 \cdot [CO_2] + 2.4 \cdot [H_2]\text{-}3.6 \cdot [H_2O]\text{-}0.5 \cdot [N_2] \qquad (3)$$

In general, nitroguanidine reduces erosion by virtue of its high nitrogen content and its lower explosion temperature.

3.6 Stability and Compatibility

The response of gun propellants to ^{198}Au (0.411 MeV)-γ-radiation has been investigated in the 1950s. **M15** propellant though exhibiting a higher gas evolution initially is surpassed after some 35 days by double-base propellants which then undergo rapid decomposition (Figure 26) [113,114].

Table 43. Measured and calculated properties of state-of-the-art gun propellants containing FOX-12 and equilibrium composition of gases based on loading density of $\Delta = 0.2\ g cm^{-3}$ [52].

Parameter	Unit	NILE	NILE-NGu	NL-100	HFR-001	EX-99	EX-99-10	EX99-20
Temperature	K	1844	1857	2744	2180	3139	2987	2833
Covolume	cm^3g^{-1}	1.208	1.217	1.086	1.190	1.120	1.123	1.125
Pressure	MPa	195.6	198.6	264.0	241.3	309.5	296.1	282.4
Force calculated	$J g^{-1}$	742	751	1033	919	1201	1148	1094
Force measured at Δ	$J g^{-1}$	895 (Δ?)						
Molecular weight	$g mol^{-1}$	20.671	20.559	22.08	19.716	21.735	21.629	21.522
Gamma	–	1.267	1.262	1.254	1.279	1.255	1.257	1.260
Equilibrium composition after *Cheetah 2.0*								
CO	Mol/Mol	0.3805	0.3620	0.2670	0.3506	0.3695	0.3592	0.3489
N_2	Mol/Mol	0.2192	0.2341	0.3000	0.2163	0.2365	0.2424	0.2482
H_2	Mol/Mol	0.2386	0.2465	0.1719	0.2847	0.2006	0.2047	0.2087
H_2O	Mol/Mol	0.0650	0.0583	0.2144	0.1100	0.1543	0.1557	0.1568
CO_2	Mol/Mol	0.0226	0.0184	0.0441	0.0228	0.0340	0.0338	0.0338
NH_3	Mol/Mol	0.0042	0.0046	0.0012	0.0038	0.0011	0.0013	0.0014
CH_4	Mol/Mol	0.0669	0.0729		0.0096			

© 2021 Wiley-VCH GmbH

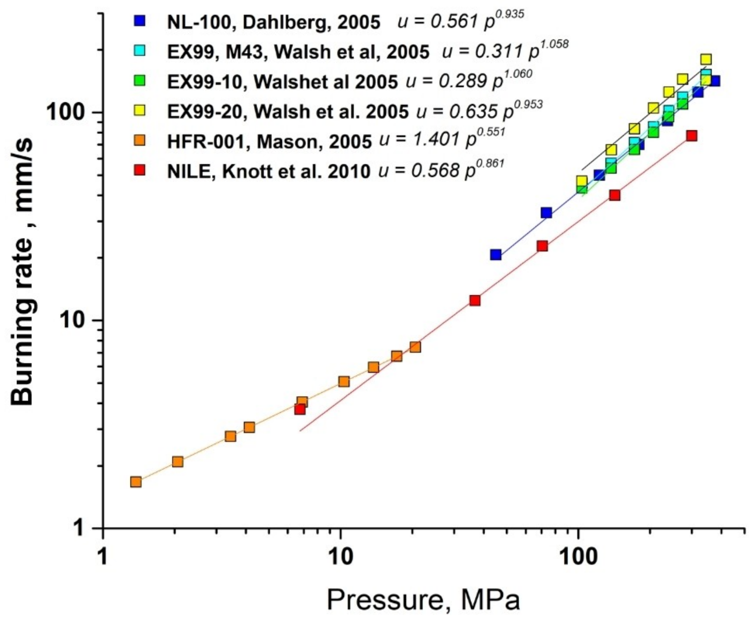

Figure 17. Burning rate of EX99 and the FOX-12 based propellants.

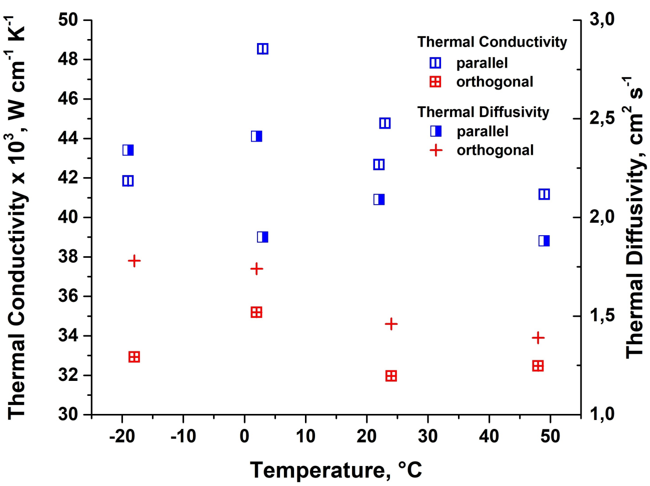

Figure 18. Thermal conductivity and diffusivity of M30 propellant parallel and orthogonal to direction of extrusion of grain [104].

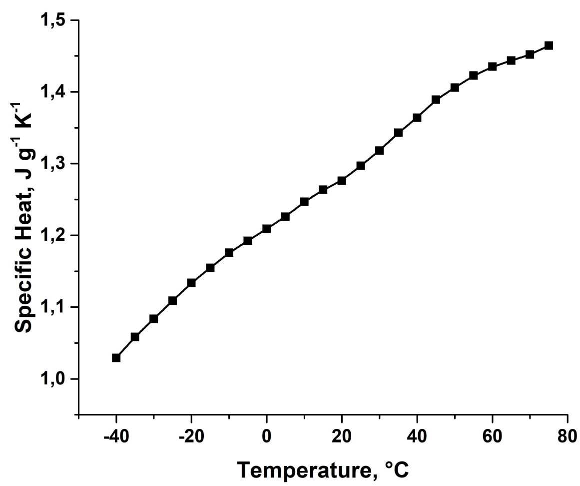

Figure 19. Specific heat of M30 propellant from Ref. [105].

Bohn has conducted many studies on the stability of energetic materials and particularly gun propellants [115, 116]. His work shows that NGu has a beneficial effect on ageing. **M30** and **Q5560** show good stability and acceptable ageing (Figurs 27 and 28).

Nitroguanidine acts as an effective stabilizer in gun and rocket propellants [117] and is compatible with many other energetic materials including nitrate esters, ammonium perchlorate (AP) [47, 118], hydrazinium nitroformate [119], TNAZ [120], DINA [121], HMX, RDX, TNT, ADN, FOX-7, FOX-12 [46]). This behaviour can be attributed to both the mild basicity of NGu [1] as well as its ability to form strong hy-

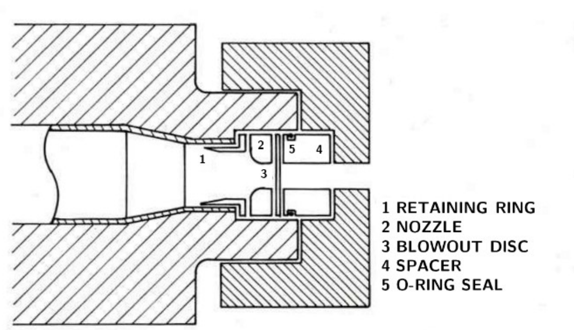

Figure 20. 37 mm Blow Out Gun after Ref. [76].

© 2021 Wiley-VCH GmbH

Table 45. Measured physical properties of M30 and TPE based propellants.

Parameter	Temperature °C	M30 47.5 wt.-% NGu	H2-HBNQ 20 wt.-% NGu	O1 24 wt.-% NGu	O3 32 wt.-% NGu
Stress at failure, MPa	21	68.9	8.14	59.89	52.33
	50	60.0	4.97	29.84	25.34
	−20	169.0	41.07	30.6	105.8
Strain at failure, %	21	3.3	12.2	13.92	12.21
	50	4	7.36	17.31	9.94
	−20	7	8.07	5.12	8.25
Modulus, GPa	21	2.26	0.0766	0.387	0.581
	50	1.6	0.0604	0.141	0.251
	−20	3.2	0.815	1.11	2.04
Failure Modulus, GPa	21	−0.26	−0.0170	0.032	0.014
	50	−0.19	−0.0127	0.082	0.071
	−20	−1.74	−0.103	−0.310	−0.603

Table 46. Average mass loss due to firings in 37 mm blow out gun at varying rupture pressure of NGu based propellants [72,76–79].

Nozzle diameter mm	Rupture pressure, MPa	Unit	*M1**	*M5*	M30	HFP	NT
17.34	193	mg/shot	*1.5*	*5.0*	2.9	3.1	
17.34	248	mg/shot			2.3		2.4
17.34	283	mg/shot	*0.8*	*25.9*	3.5	7.1	
17.34	413	mg/shot	–	*116.4*	23.8	42.9	
12.4	250	mg/shot			3.9		
12.5	274	mg/shot			21.1		
6.4	250	mg/shot			67.7		

*Single Base reference gun propellant.

Table 47. Erosivity [65].

Propellant	*M1*	*M5*	*HG*	HUG
Erosivity g/g	*50*	*100*	*115*	80

Table 48. Average mass loss due to firings in 37 mm blow out gun at varying rupture pressure of NGu based propellants [76–79,97].

Parameter	Unit	*M1**	*M5*	Q5560	KHP-212
Surface erosion	µm/shot	*0.1070*	*1.6249*	0.2905	0.0961
Edge erosion	µm/shot	*0.1251*	*9.2744*	0.9069	0.2445

*Single Base reference gun propellant.

Table 49. Mass loss due to erosion after Ref. [109].

Propellant	*NK1280*	M30	*M39*	NL-100
Erosion (g)	0.340	0.257	*0.251*	0.206

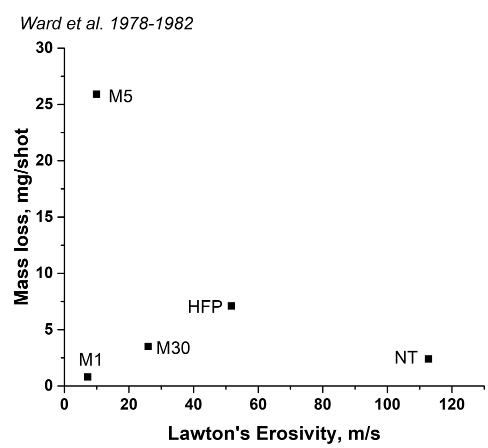

Figure 21. *Lawton's* erosivity [112] versus experimental erosivities for gun propellants reported by *Ward* [76–79].

drogen bonds stabilizing other covalent or ionic compounds [1].

On the contrary, the compatibility of guanylurea dinitramide (FOX-12) with other energetic materials is scarcely published and the very few disclosed findings do not encourage its use. In combination with RDX, FOX-12 lowers the decomposition temperature of RDX [122] hence render-

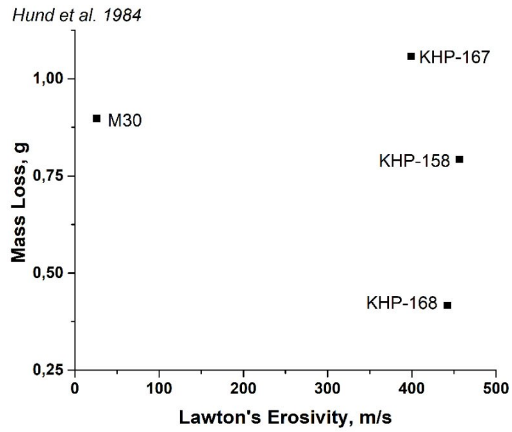

Figure 22. *Lawton's* erosivity [112] versus experimental erosivities for gun propellants reported by *Hund et al.* [142].

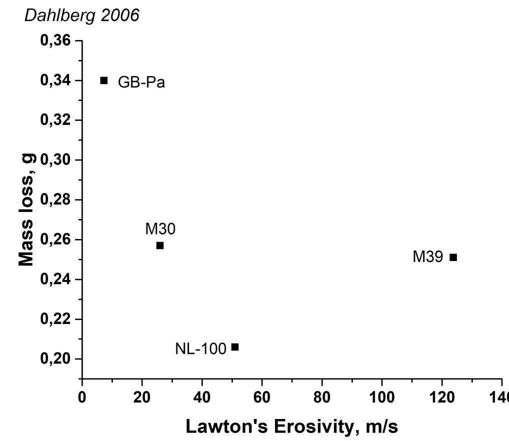

Figure 25. *Lawton's* erosivity [112] versus experimental erosivities for gun propellants reported by *Dahlberg* [99].

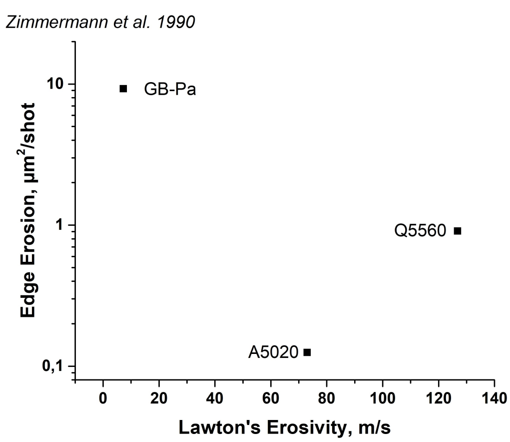

Figure 23. *Lawton's* erosivity [112] versus experimental erosivities for gun propellants reported by *Zimmermann et al.* [96–97].

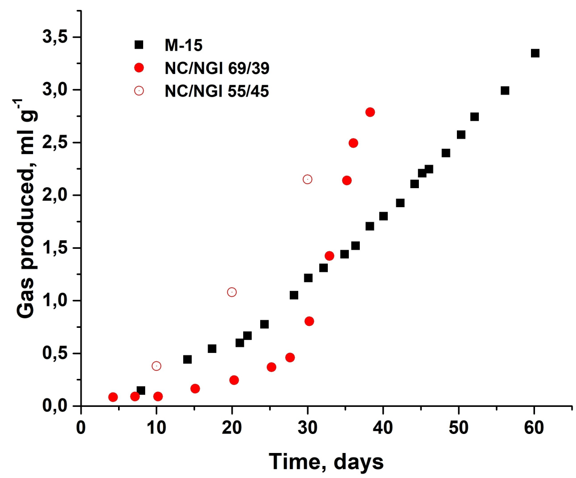

Figure 26. Gas evolution of **M15** propellant in comparison to double base powders [113].

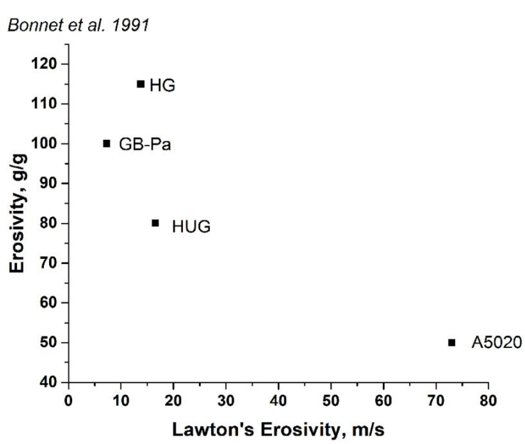

Figure 24. *Lawton's* erosivity [112] versus experimental erosivities for gun propellants reported by *Bonnet et al.* [65].

ing the stability of such sort of propellant (**NL-100** or **NILE**) precarious. In a similar fashion, FOX-12 lowers the thermal stability of AP based propellants [34].

3.7 Sensitiveness and IM-Signature

Though nitroguanidine and FOX-12 are similar insensitive energetic materials, NGu, by virtue of its fibrous nature, is also able to impart mechanical rigidity into a composite propellant grain as has been found by *Fong and Warren* by the elucidation of an interphasic region between NGu and nitrocellulose. This yields a unique low mechanical sensitiveness of **M30** gun propellant when compared with those propellants containing other non fibrous energetic fillers [123]. In addition, the high aspect ratio of NGu crystals through orientation of the fibres along the axis of extrusion

© 2021 Wiley-VCH GmbH

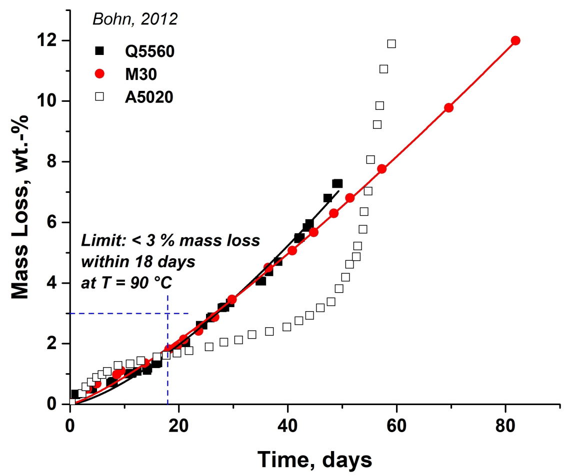

Figure 27. Mass loss of two NGu-based propellants at 90 °C compared to single base **A5020**.

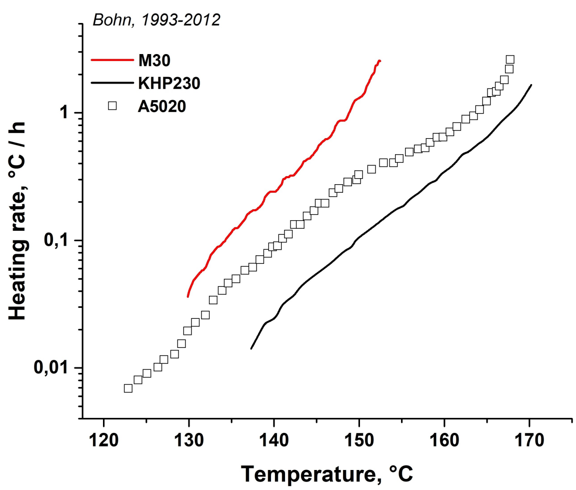

Figure 28. Adiabatic Self-heating of two NGu based propellants compared to **A5020**.

[68] also adds to the reduced impact sensitiveness of this propellant [124–127]. The influence of process parameters on M30 propellant sensitiveness is discussed in Ref. [128]. Table 50–53 summarize the sensitiveness of NGu-based propellants.

A study of the radiative heating and ignition of **HUX** propellant has been reported by *Della Pieta et al.* in Ref. [129].

Andersen et al. determined the impact ignition threshold and type of reaction for **M30** at three different calibres, 5.56 mm (.22 cal), 6.5 mm (.257 cal), and 12.7 mm (.50 cal) which is depicted in Figure 29 [130,131].

Baschung and *Grune* determined the critical diameter and shock sensitivity of **M30** and **MTLS** propellants in accordance with German and French standards (Table 54, 55) [98].

Frey and *Rocchio et al.* have investigated the cookoff behaviour of **M30** propellants [132,133] (Figure 30). *Nguyen* and *Berry* have tested **M30** among other propellants with the hot fragment conductive ignition test (Figure 31) [134].

To model the response of **M30** to shock, the Hugoniot for porous **M30** propellant has been determined by *Boyle* (Figure 32 and 33) [136].

3.8 Deflagration to Detonation Transition (DDT)

M15 and **M30** propellants have been tested for DDT by internal ignition in both 12-inch and 24-inch long pipe bombs. **M30** propellant yields about seven times as many fragments as **M15**, which is indicative of a fiercer reaction under confinement, which is due to the high content in both NGl and NC (Table 56).

The IM signature of **M30** [137], **MTLS**, **NILE** [138], and **HUX** propellant in their respective munition configurations is given in Table 57.

Petino [139] investigated the dust explosion sensitivity of M-30 propellant.

Table 50. Sensitiveness of experimental NGu-based gun propellants compared to pure RDX.

Test	Unit	M15	M30	MTLS	HUX	MRCA	*RDX Class 5*
	Alternative Designations	N6060	N6540 IN5340 H1600	R5730	H1707	Q5560	
BAM-Friction	N			160			120
ABL-Friction	Psig						100
BAM-Impact	J			15			7.5
ERL-Impact	mm	183±4.5	162±3.6				
NOS-Impact	mm	183					196
DSC onset	°C	170	157				204
T_i	°C	167	169	170		168-172	
E_A	kJ mol^{-1}	172.8	195.0				
$T_{ex\ 5s}$	°C	231	212				
Koenen	mm			8			8

© 2021 Wiley-VCH GmbH

Table 51. Sensitiveness of experimental NGu based gun propellants [98].

Test	Unit	HUG	NENA NQ20	NENA NQ40
	Alternative Designations			
Density	$g\,cm^{-3}$			
BAM-Friction	N	204	288	252
ABL-Friction	Psig			
BAM-Impact	J	6	12.3	9.8
T_i	°C	171	181	182

Table 52. Sensitiveness of gun propellants based on FOX-12 [83,109].

Test	Unit	NILE	NL-100	HFR
ABL-Friction	Psig	560		
NOS-Impact	cm	35,5		100

Table 53. Sensitiveness of experimental NGu-based gun propellants [71–73].

Test	Unit	O-1	O-3	H-2	H-2(HBNQ)
BAM-Friction	N			288	240
ABL-Friction	Psig	800	800		
ERL-Impact	cm	87.8	>100	>240	118
ABL-Impact	cm	21	51		
SBAT onset	°C	151	151		

Though NGu has higher explosive energy than FOX-12, it can be easily desensitized by wetting with ≥20 wt.-% water to give a material which is characterised as a flammable solid only, HD 4.1. FOX-12 on the other hand cannot be desensitized in the same manner. On the contrary, the much higher pressure exponent for pure low-density FOX-12 indicates a greater likeliness to undergo DDT upon combustion.

Table 54. Critical diameter of **M30** and **MTLS** gun propellant and type of reaction in gap test [115].

Formulation	Mass (kg)	Critical Diameter (mm)	Reaction type*	Reaction velocity ($m\,s^{-1}$)
M30	>0.6	⩾80	III	3400
			IV	2400
MTLS	>1.5	>50	V	–

*) in accordance with AOP-39.

Table 55. Response to shaped charge jet impact on **M30** and **MTLS** [98].

Formulation	Mass (kg)	Configuration	Reaction type
M30	3.5	Steel pipe 80 mm diameter, −40 °C	III
	3.5	Steel pipe 80 mm diameter, 21 °C	III/IV
MTLS	2.8	DM 72 Unit charge MTLS in logistical packaging	V

4 Combustible Cartridge Cases

Nitroguanidine has been investigated as an energetic filler in combustible cartridge cases both with NC and BAMO

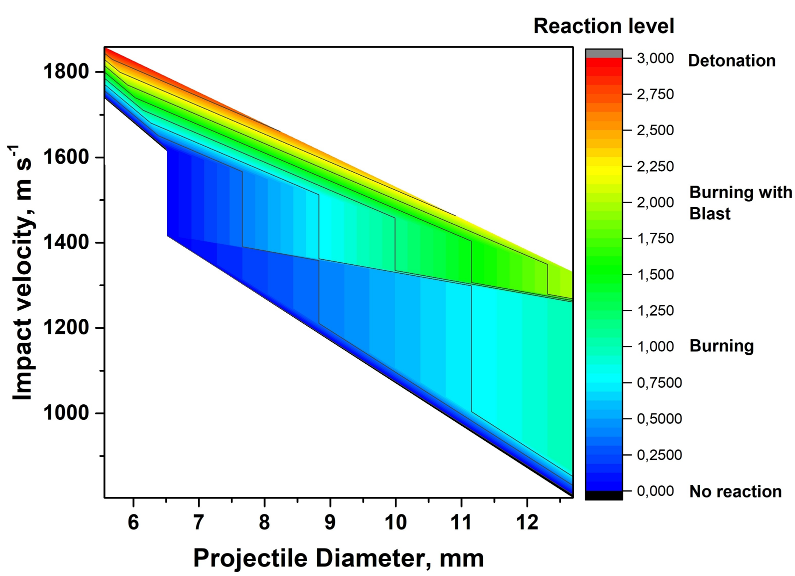

Figure 29. Impact reaction levels of **M30** propellant from Ref. [130,131].

 © 2021 Wiley-VCH GmbH

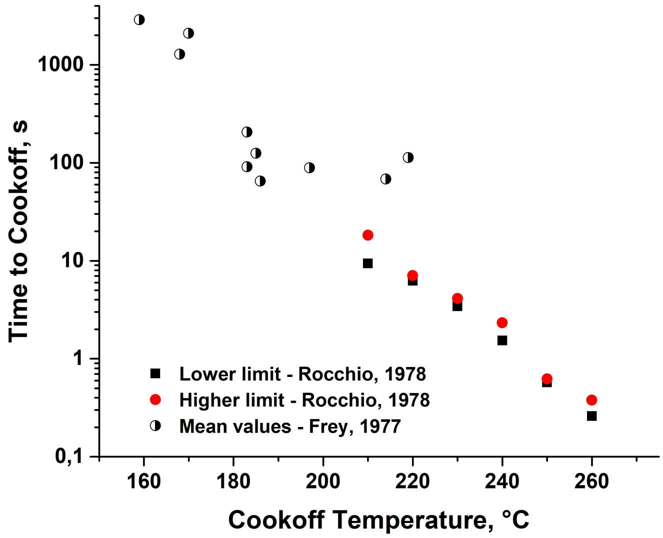

Figure 30. **M30**-cookoff temperature versus time from *Frey (1977)* and *Rocchio (1978)*.

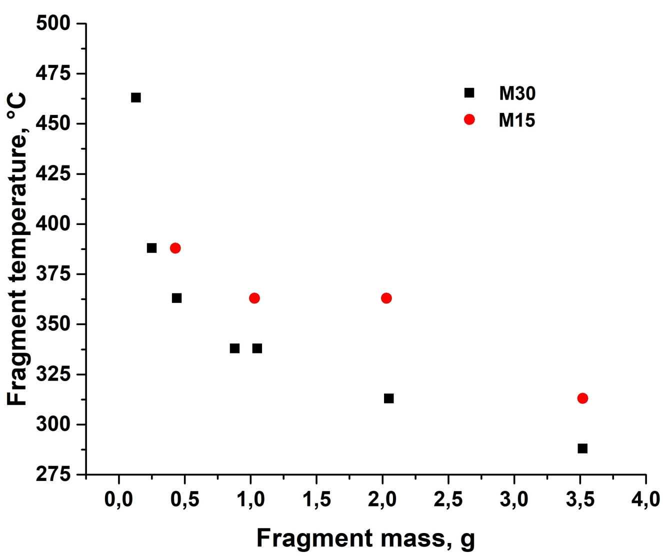

Figure 31. Fragment ignition temperature versus fragment mass for **M15** and **M30** propellants from *Kirshenbaum* (1983) [135] and *Nguyen* (1994) [134].

binder [140,141]. NGu increases the burning rate of NC/cellulose system as is depicted in Table 58.

An increase in force can be achieved by replacing NC/Cellulose with BAMO [140]. A formulation containing 20 wt.-% NGu and 80 wt.-% BAMO burns in the pressure range between 7–100 MPa, $u = 7.21\ p^{0.441}$ (Table 59).

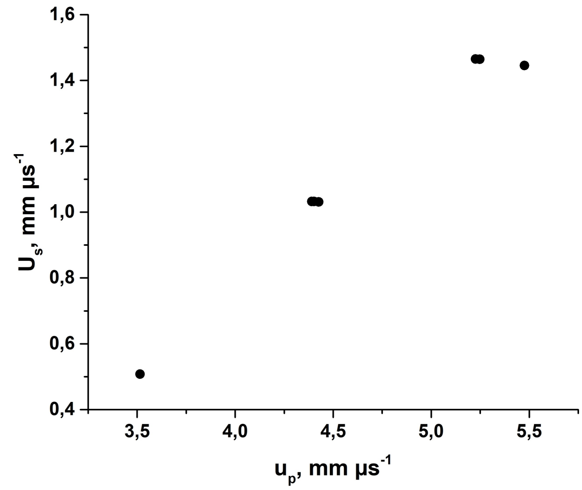

Figure 32. Hugoniot data U_s-u_p plane for **M30** propellant [136].

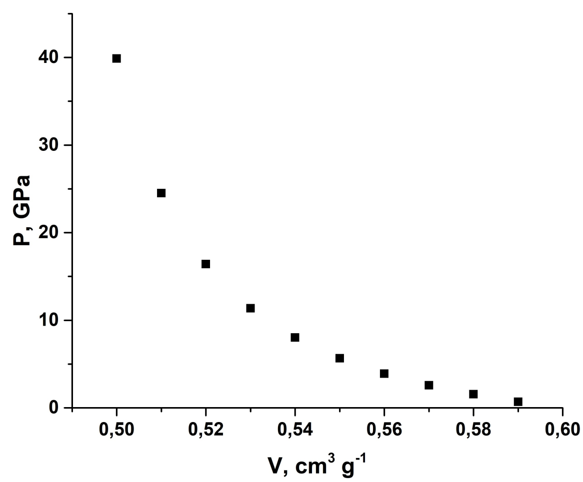

Figure 33. Hugoniot data *v-p* plane for **M30** propellant [136].

Table 56. Fragmentation of **M15** and **M30** propellants in pipe bomb test [135].

Propellant	Average loading density g cm^{-3}		Average time to rupture ms		Average number of fragments -	
Configuration	12 inch	24 inch	12 inch	24 inch	12 inch	24 inch
M15	0.777	0.678	2.57	3.51	2.5	5.5
M30	0.798	0.761	3.54	–	6.5	37.3

5 Conclusion and Outlook

Nitroguanidine is a versatile ingredient for insensitive, gun-, rocket-, base bleed, and gas generator propellant. Gun propellant formulations containing NGu show relatively low combustion/explosion temperatures with only minimum

© 2021 Wiley-VCH GmbH

Table 57. IM Signature of munitions containing either NGu- or FOX-12 based gun propellants.

Propellant	Configuration	SH*	FH*	FI*	BI*	SCJI*	SR*
M30	Steel pie	IV	IV		III	V III	III
MTLS	DM72 Unit charge		V V	V V	V V	V IV/V	V NR
HUX	Brass cylinder	IV	V V	IV	IV		V III
NL-100	Uniflex CCC	V V	V V	V IV	V NR	V IV	V V
NILE [59]	155 mm brass cartridge	V V		V III			
503	STANAG 4526					V V	
516	STANAG 4526					V NR	
519	STANAG 4526					V V	
512	STANAG 4526					V NR	

*Reaction types in accordance with AOP-39.

Table 58. Formulation of experimental CCC [140, 141].

	Unit	C-1	C-2	C-3	C-4	C-5
NC (12.6)	wt.-%	70	65	60	55	50
NGu	wt.-%	15	20	25	30	35
Cellulose	wt.-%	15	15	15	15	15
DBP	wt.-%	+3.5	+3.5	+3.5	+3.5	+3.5
DPA	wt-%	+1	+1	+1	+1	+1
Burning rate	a.u.	1	1.155	1.280	1.907	2.522

Table 59. The mechanical properties BAMO/NGu (80/20) at 20 °C [140].

Parameter		
Modulus	MPa	83.426
Strain at Max Stress	%	15.8
Strain at failure	%	138
Max Stress	MPa	6.529

muzzle flash and also reduced erosion. Their performance spans from very lean formulations giving some $f = 750$ J/g up to $f = 1320$ J/g when formulations contain extra RDX and an energetic binder of the GAP-type. In rocket propellants and combination with oxidizers (AP or ADN), specific impulses range from 185–267 s. NGu-based propellants by virtue of the fibrous nature of NGu are mechanically rigid, only mildly sensitive to impact and yield favorable IM signature. The weak basicity of NGu and its strong hydrogen bonds are the origin for an unmatched thermal stabilization and desensitization of formulations containing a other energetic materials.

It is this array of advantageous properties combined with its sustainable production and its inexpensive nature which makes nitroguandine the high nitrogen compound of choice for the formulation of todays and tomorrows propellants.

Abbreviations

Ω	Oxygen balance, wt.-%
γ	Ratio of specific heats
N	Nitrogen content, wt.-%
m_r	Molecular weight, g mol^{-1}
M	Mean Molecular weight, g mol^{-1}
ρ	Density, g cm^{-3}
Δ	Loading Density, g cm^{-3}
$\Delta_f H$	Enthalpy of formation, kJ mol^{-1}
Mp	Melting point, °C
T_{dec}	Decomposition temperature, °C
$\Delta_{ex}H$	Explosion enthalpy, kJ mol^{-1}
f	Force, J g^{-1}
c_p	Specific heat at constant pressure, J g^{-1} K^{-1}
c_L	Longitudinal speed of sound, m s^{-1}
κ	Thermal conductivity, W m^{-1} K^{-1}
S	Solubility, g kg^{-1}
ARC	Accelerated Rate Calorimetry Onset, °C
V_D	Detonation velocity, m s^{-1}
P_{CJ}	Detonation pressure, GPa
$\sqrt{2E_G}$	Gurney Energy, ms^{-1}
ADN	Ammonium dinitramide, $H_4N_4O_4$
AMMO	3-Azidomethyl-3-methyloxetan, $C_5H_9N_3O$
AN	Ammonium nitrate, $H_4N_2O_3$
AP	Ammonium perchlorate, ClH_4NO_4
BAMO	3,3-Bis(Azidomethyl)oxetan, $C_5H_8N_6O$
BDNPA	Bisdinitropropylacetal, $C_8H_{14}N_4O_{10}$
BDNPF	Bisdinitropropylformal, $C_7H_{12}N_4O_{10}$
BI	Bullet Impact
CCC	Combustible Cartridge Case
DEG(D)N	Diethylenglycol dinitrate, $C_4N_8N_2O_7$
DNDA-5,6	Blend of three Dinitrodiaza alkanes, $C_{36}H_{92}N_{40}O_{40}$
EC	Ethylcentralite, $C_{17}H_{20}N_2O$
FH	Fast heating
FI	Fragment Impact
FTIR	Fourier Transform Infrared
GAP	Glycidyl azide polymer, $[C_5H_5N_3O]_n$
GUDN	Guanylurea dinitramide (FOX-12), $C_2H_7N_7O_5$
GUDOL	Nitroguanidine -NC-DEGN-based propellants
HBNQ	High Bulk density Nitroguanidine
HTPB	Hydroxyl terminated Polybutadiene
KHP	Cold High Performance Powders (Ger: ***K**alte **H**ochleistungs**P**ulver*)
MRCA	Multi Role Combat Aircraft
MTLS	Modular Charge system (Ger: ***M**odulares **T**reib**La**dungs**S**ystem*)
NC	Nitrocellulose
NE	Nitrate Ester (e.g. nitrogylcerine, diethylene glycol dinitrate, etc.)
NGl	Nitroglycerine, $C_3H_5N_4O_9$
NGu	Nitroguanidine, $CH_4N_4O_2$
NILE	Navy Insensitive Low Erosion
PTFE	Polytetrafluorethylene, $[C_2F_4]_n$
RDX	Hexogen, $C_3H_6N_6O_6$
SCJI	Shaped Charge Jet Impact

 © 2021 Wiley-VCH GmbH

SH	Slow Heating
SR	Sympathetic Reaction
TEGDN	Triethylen glycol dinitrate, $C_6H_{12}N_2O_8$
TPE	Thermoplastic Elastomer
TSE	Twin Screw Extrusion
UV-VIS	Ultraviolet-Visible
WASAG	Westfälisch-Anhaltische Sprengstoff-Actien-Gesellschaft (1891-2001)

Acknowledgement

The author thanks *Dr. Alexander Huber*, Nitrochemie, Aschau am Inn, Germany for helpful information and insights on German NGu-based propellant developments. *Dr. Ernest Baker (Technical Specialist Officer (TSO)-Warhead, Martijn van der Voort (TSO - Munitions Transport and Storage)* both at the NATO-Munitions Safety Information Analysis Center (MSIAC), Brussels, Belgium and *Dr. Matt Andrews (formerly TSO-Energetic Materials, MSIAC, now with DOSG, United Kingdom)* are thanked for answering technical questions (TQs: 2020-DEU-2948, 2018-DEU-2787) and further helpful discussions on nitroguanidine. *Dr. Manfred Bohn*, Fraunhofer ICT is thanked for helpful information and discussion on stability of NGu based propellants. The author thanks Fraunhofer ICT and French-German ISL for provision of copies of scientific reports [4] and [97] respectively. The author is also indebted to the two referees for their detailed critical review and the many suggestions that greatly helped improve this paper. The author gratefully acknowledges *AlzChem Trostberg GmbH*, Trostberg, Germany for funding this work.

Data Availability Statement

All data has been made available

References

[1] E.-C. Koch, Insensitive High Explosives: III. Nitroguanidine-Synthesis-Structure-Spectroscopy-Sensitiveness, *Propellants Explos. Pyrotech.* **2019**, *44*, 267–292.

[2] E.-C. Koch, Insensitive High Explosives: IV. Nitroguanidine-Initiation & Detonation, *Def. Tech.* **2019**, *15*, 467–487.

[3] R. L. Simmons, C. M. Walsh, Designing Advanced Gun Propellants with Improved Energy Release, *32nd International Annual Conference of the Fraunhofer ICT* July 3–6, **2001**, Karlsruhe, Germany 43–1–43–11.

[4] F. Volk, J. Klink, K. Mozer, *Das Verhalten von Nitroguanidin bei der thermischen Zersetzung, Bericht 2/83*, Fraunhofer-Institut für Treib- und Explosivstoffe, Pfinztal, **1983**, 61 pp.

[5] S. Gordon, B. J. McBride, Computer Program for Calculation of Complex Chemical Equilibrium Compositions and Applications, *NASA Reference Publication 1311*, NASA, Cleveland, OH, October **1994**, 55p.

[6] A. P. Glazkova, Effect of Catalysts on the Combustion of Nitroguanidine and Ammonium nitrate-Nitroguanidine Mixtures, *Combustion Explosion Shock Wave*, **1971**, *7* 177–185.

[7] A. P. Glazkova, Catalysis in Deflagration of Explosives, *Explosivstoffe*, **1973**, *21*, 137–145.

[8] A. P. Glazkova, The Effect of Catalysts on the Combustion of Explosives, *Combustion Explosion Shock Wave*, **1974**, *10*, 281–290.

[9] U. Bemm, H. Östmark, H. Bergmann, A. Langlet, FOX-12, A New Energetic Material with Low Sensitivity for Propellants and Explosives Applications, *IMEMTS*, Reno, NE, USA, **1998**, VB-4-1–VB4–10.

[10] D. McAteer, J. Akhavan, A. Contini, The development of novel, low sensitivity, gas-generating formulations for hotwire ignited devices, *NTREM* **2014**, Pardubice, Czech republic, 323–336.

[11] P. G. Butts, C. R. Fingerhood, *Gas-Generating Compositions*, US3123507, USA, **1964**.

[12] D. R. Poole, G. F. Holland, N. A. Wolf, M. A. Wilson, *Thermally stable gas generating composition*, US5545272, USA, **1996**.

[13] A. I. Lesnikovich, Negative Correlation of Combustion Rate Law Parameters, *Combustion Explosion Shock Waves*, **1979**, *15*, 30–34.

[14] H. R. Blomquist, *Apparatus comprising an inflatable vehicle occupant protection device and a gas generating composition therefor*, US 6,004,410, USA, **1999**.

[15] E.-C. Koch, *unpublished results*, **2008**.

[16] K. Engelen, M. H. Lefebvre, J. de Ruyck, Chemical formulation of solid propellants for specific gas generators, *24th Int. Pyrotechnics Sem.* **1998**, Monterey, CA, USA, 203–216.

[17] K. Engelen, L. Vanneste, M. H. Lefebvre, Influence of the particle size on the combustion properties of a pyrotechnic mixture, *28th Int. Pyrotechnics Sem.* **2001**, Adelaide, Australia, 263–271.

[18] K. Engelen, M. H. Lefebvre, A. Hubin, Properties of a Gas-Generating Composition related to the Particle Size of Oxidizer, *Propellants Explos. Pyrotech.* **2002**, *27*, 290–299.

[19] K. Engelen, M. H. Lefebvre, Properties of Gas-Generating Mixtures related to different Fuel and Oxidizer Compositions, *Propellants Explos. Pyrotech.* **2003**, *28*, 201–209.

[20] C.-Y. Cao, S. Lu, D. Zhang, L.-L. Gong, H.-P. Zhang, Effects of nitroguanidine on the thermal behavior and burning characteristics of 5-amino-1*H*-tetrazole-based propellants, *RSC Adv.* **2017**, *7*, 13808–13816.

[21] E. W. Price, H. B. Mathes, B. A. Sword, H. J. Sprouse, Axial Mode Combustion Instability in Solid Propellant Rocket Motors, *NAVWEPS Report 8658, NOTS, TP 3700*, December **1964**, US Naval Ordnance Test Station, China Lake, CA, USA; declassified 22 Mai **1980**.

[22] H. C. Allen, M. T. Cucksee, *The Effects of an immiscible binder component on the rheological and mechanical properties of a composite solid propellant*, US Army Missile Research and Development Command, Redstone, AL, USA, June **1978**, 15 pp.

[23] B. J. Kim, M. R. Kemme, B. K. Gullett, R. K. Williams, J. M. Aurell, Innovative Technology Development for Comprehensive Air Quality Characterization from Open Burning, *SERDP WP-2153*, Final Report, April **2012**, 108 pp.

[24] J. Philipson, *Slow Burning Solid Composite Propellant*, US3031347, USA, **1962**.

[25] E. Genter, P. Semmler, *Verfahren zum Anzünden eines Raketenfeststofftriebwerkes*, DE2128243, Germany, **1973**.

[26] K. Klager, *Sustainer Propellant*, GB 1605257, USA, **1986**.

[27] P. J. Blatz, D. A. McQuarrie, M. C. Shen, On the simple tensile deformation of an incompressible rubber matrix filled with non-adherent rigid spheres of uniform size distribution, *Interagency Chemical Rocket Propulsion Group, Mechanical Behavior Working Group 5th Meeting. Vol I*, Chemical Propulsion Information Agency, Silver Spring, MD, pp 121–131, **1966**. Accessed at on July 9 2020 at https://authors.library.caltech.edu/62432/.

[28] Solid Propellant Smoke Classification, STANAG 6016, NATO Military Agency for Standardization, Brussels, June **1996**, 16 pp.

© 2021 Wiley-VCH GmbH

[29] M. Liljedahl, J. Ritums, H. Östmark, FOX-12: From Synthesis to IM-Application, *48th International Annual Conference of the Fraunhofer ICT*, Karlsruhe, Germany, June 27–30, **2017**, V22.
[30] N. Wingborg, A. Lindborg, C. Oscarson, M. Sjöblom, Characterization of solid propellants based on ADN and GAP, AIAA 2015–4222, *51st AIAA/SAE/ASEE Joint Propulsion Conference*, Orlando FL, USA, 25–27 July **2015**.
[31] N. Wingborg, M. Skarstind, M. Sjöblom, A. Lindborg, M. Brantlind, J. Johansson, S. Ek, M. Liljedahl, J. Kjellberg, Ammonium dinitramide, *50th International Annual Conference of the Fraunhofer ICT*, June, 25–28, **2019**, Karlsruhe, Germany.
[32] M. K. Hadhoud, M. A. Radwan, M. A. Sadek, S. M. Abdelkarim, Performance Characteristics of Nitramine Rocket Propellants, *24th International Annual Conference of the Fraunhofer ICT*, 29 June-2 July **1993**, Karlsruhe, Germany, V-43.
[33] K. Kuhn, T. Netzer, *Silicone Propellant Compositions Containing Nitroguanidine*, US3197349, Germany, **1965**.
[34] H. Xu, F. Zhao, W. Pang, Y. Li, J. Yang, Z. Liu, Properties of high burning rate HTPB propellant containing FOX-12, *J. Solid Rocket Tech.* **2011**, *34*, 745–749.
[35] Y. Li, J. Wang, The Real-Time Diagnostics of Combustion Characteristics of Solid Propellant by Remote Sensing FTIR System, *Instrument. Sci. Tech.* **2003**, *31*, 33–45.
[36] J. Lipkin, C. Shaddix, S. Allendorf, R. Peabody, C. Velsko, B. Watkins, S. Williams, A. Moeller, W. Bellow, J. Carson, W. Gray, J. Stephens, S. Kwak, Contained low-pressure combustion of Nike and improved Hawk Rocket Motors: Experimental Techniques and emissions measurements, *International Journal of Energetic Materials and Chemical Propulsion*, **2002**, *5*, 40–49.
[37] T. H. Pratt, Comparative tests of propellants by peak side-on overpressure and side-on impulse, *Technical Report S-148*, U. S. Army Missile Command Redstone Arsenal, AL, USA, 90 pp, October **1967**; declassified 31 Dec **1973**.
[38] R. F. Vetter, Missile Systems propulsion Cook-Off, *17th DDESB Explosives Safety Seminar*, Denver, CO, USA, 14–16. September **1976**, 1011–1014.
[39] L. B. Jensen, H. P. Marshall, Response of some Polyurethanes to humid environment, *Conference: Compatibility of Propellants, Explosives and Pyrotechnics with Plastics and Additives*, Picatinny Arsenal, Dover NJ, USA, December 3–4 **1974**, III–E-1–12.
[40] W. Klöhn, D. H. Müller, H. Schubert, *Treibstoff für Base-Bleed-Gasgeneratoren, Verfahren zu seiner Herstellung sowie zur Herstellung eines Treibsatzes aus diesem Treibstoff*, DE3006475 C2, Germany, **1986**.
[41] W. Klöhn, A. Rassinfosse, Base-Bleed-Festtreibstoffe mit thermoplastischen Elastomeren als Binder, *12th International Annual Conference of the Fraunhofer ICT*, 1–3 July, Karlsruhe, Germany, **1981**, 289–304.
[42] H. F. R. Schöyer, P. A. O. G. Korting, Combustion of Composite Propellant at extremely low pressures, *13th International Annual Conference of the Fraunhofer ICT*, Karlsruhe, Germany, June 30–2 July **1982**, 207–227.
[43] H. F. R. Schöyer, P. A. O. G. Korting, Propellant Combustion at Low Pressures, *Combust. Flame*, **1986**, *63*, 317–327.
[44] H. F. R. Schöyer, P. A. O. G. Korting, Low Pressure Combustion of Composite Propellant, *Propellants Explos. Pyrotech.* **1984**, *9*, 149–156.
[45] S. Zeuner, A. Hofmann, R. Schropp, K.-H. Rödig, *Particle-Free, Gas-Producing Mixture*, US5989367, Germany, **1999**.
[46] G. K. Lund, *Gas Generation via Elemental Carbon-Based Composition*, US8980023, USA, **2015**.
[47] R. Li, X. Guo, J. Zhang, H. Zhang, C. Wu, Investigation on the Thermal Behavior of Nitroguanidine, Potassium Perchlorate, Ammonium Perchlorate and their Mixtures by DSC and TG, *3rd Int. Conf. on Infor. Tech. Indust. Autom.* **2018**, 298–307.
[48] S. Eisele, K. Menke, Gasgenerator propellants based on GUDN, *41st International Annual Conference of the Fraunhofer ICT*, June 29- July 2, **2010**, Karlsruhe, Germany, V43.
[49] K. Menke, S. Eisele, *Gasgenerator-Treibstoffzusammensetzung, Verfahren zu ihrer Herstellung und deren Verwendung*, DE102011100113A1, Deutschland, **2012**.
[50] K. Menke, J. Neutz, U. Schleicher, Pyrotechnische Kaltgasgeneratoren als Bestandteil von Unterwasser-Rettungssystemen für U-Boote und Tauchplattformen, in *Wehrwissenschaftliche Forschung Jahresbericht 2011 Innovative Verteidigungsforschung für ein zukunftsorientiertes Fähigkeitsprofil der deutschen Streitkräfte 11*, Bundesministerium der Verteidigung, Bonn, April 2012, S. 28–29.
[51] K. Menke, J. Neutz, U. Schleicher, *Pyrotechnische Kaltgasgeneratoren*, DE102012217718 A1, Deutschland, **2013**.
[52] L. E. Fried, W. M. Howard, P. C. Souers, *Cheetah 2.0*, Lawrence Livermore National Laboratory, **1998**.
[53] H. Flemming, Stabilmachen von Schießbaumwolle, *Angew. Chem.* **1898**, *11*, 1053.
[54] P. Vieille, Etude sur les phenomenes d'erosion produit par les explosifs, *Mem. Poudr. Salp.* **1900**, *11*, 157–219.
[55] M. Abelli, *Smokeless Explosive*, US Patent 899.855, **1908**, Italy.
[56] J. N. Pring, *Flashless Propellants*, Ministry of Supply, UK, **1948**, 131 pp.
[57] B. T. Fedoroff, A. A. Aaronson, G. D. Clift, E. F. Reese, *Dictionary of Explosives, Ammunition, and Weapons*, Picatinny Arsenal, Dover, NJ, **1958**, Ger-149.
[58] U. Gallwitz, *Die Geschützladung*, J. Neumann-Neudamm, **1944**, p. 156; p. 152.
[59] A. Huber, Nitrochemie Aschau, Germany, *personal communication*, August **2020**.
[60] U. Sirringhaus, *Explosivstoff-Datenbank, Version 4.1*, Wehrwissenschaftliches Institut für Werk-, Explosiv und Betriebsstoffe, Swisttal-Heimerzheim, **2008**.
[61] U. Proksch-Jeck, *Dreibasiges Treibladungspulver*, DE09102468-U1, Deutschland, **1990**.
[62] U. Proksch-Jeck, Propellant development for insensitive ammunitions, *ADPA-Meeting, Joint international Symposium on Energetic Materials Technology*, 5–7 October **1992**, USA. pp. 122–27.
[63] H. Brachert, D. Gerke, J. Kleiß, *Verfahren zur Herstellung von Gudol-Pulver*, DE2316538, Deutschland, **1974**.
[64] H. Brachert, D. Gerke, G. Kellner, *Ein- oder mehrbasiger Pulverkörper für Treibladungen und Verfahren zu ihrer Herstellung*, DE2520882 C1, Deutschland, **1986**.
[65] B. Bonnet, J.-M. Paindavoine, J.-L. Paulin, M. Rat, High Energy NC-based propellant properties for Large Caliber Gun, *5th Int. Gun Propellant and Propulsion Symposium*, Picatinny Arsenal, NJ, USA, Nov. **1991**, II-88–II-96.
[66] J. Suuronen, TEGDN, Sensitivity reducing ingredient for nitrocellulose based propellants, *IMEMTS*, October 11–14, **2010**, Munich.
[67] F. Schedlbauer, LOVA Gun Propellants with GAP binder, *Propellants Explos. Pyrotech.* **1992**, *17*, 164–171.
[68] F. Volk, H. Bathelt, Influence of Energetic Materials on the Energy-Output of Gun Propellants, *Propellants Explos. Pyrotech.* **1997**, *22*, 120–124.
[69] F. Volk, H. Bathelt, Performance Parameters of Explosives: Equilibrium and Non-Equilibrium Reactions, *Propellants Explos. Pyrotech.* **2002**, *27*, 136–141.
[70] H. Ritter, B. Baschung, P. Franco, Increase of Gun performance using Co-layered propellants based on Nena Formulations,

 © 2021 Wiley-VCH GmbH

38th International Annual Conference of the Fraunhofer ICT, Karlsruhe, DE, June 26 - June 29, **2007**, V-16.

[71] P. Braithwaite, D. Backes, A. Haaland, R. B. Wardle, T. Manning, L. Harris, K. Klingaman, Characterization of Thermoplastic-Elastomer (TPE) Gun Propellants, *IMEMTS*, **1999**, 92–100.

[72] C. S. Leveritt, P. J. Conroy, A. W. Johnson, Relative Erosivity of Nitramine Gun Propellants with Thermoplastic/Elastomer binder systems, *10th U. S. Army Gun Dynamics Symposium*, **2001**, 258–264.

[73] L. E. Harris, T. Manning, K. Klingaman, R. B. Wardle, J. P. Braithwaite, G. W. Dixon, T. Stephens, S. Prickett, Thermoplastic Elastomer (TPE) Gun Propellant, *IMEMTS*, IIB-2-1–14, **1998**.

[74] M. J. Penney, A. M. Wilton, T. W. D. Somerville, *Insensitive Munition Propellants*, US Patent 9,919,980; UK, **2018**.

[75] F. Volk, D. Mueller, Investigation of Gun Propellants with New Energetic Plasticizers, *24th International Pyrotechnics Seminar*, Chicago, IL, USA, **1998**, pp. 543–552.

[76] R. W. Geene, J. R. Ward, T. L. Brousseau, A. Niiler, R. Birkmire, J. J. Rocchio, Erosivity of a Nitramine Propellant, *ARBRL-TR-02094*, Aberdeen, MD, USA, August **1978**, 29 pp.

[77] J. R. Ward, R. W. Geene, Erosivity of a nitramine propellant with a flame temperature comparable to M30 propellant, *ARBRL-TR-02926*, Aberdeen, MD, USA, June **1979**, 34 pp.

[78] R. P. Kaste, I. C. Stobie, J. R. Ward, B. D. Bensinger, Relative Erosivity of Nitramine, Triple-Base, and Double Base Propellants, *ARBRL-TR-02339*, Aberdeen, MD, USA, June **1981**, 38 pp.

[79] J. R. Ward, T. L. Brousseau, R. P. Kaste, I. C. Stobie, B. Bensinger, Erosivity of Lova Propellants, *ARBRL-TR-02368*, Aberdeen, MD, USA, September **1981**, 23 pp.

[80] B. Gustafsson, J. Dahlberg, P. Sjöberg, New Insensitive Modular Charge Based on GUDN, *36th International Annual Conference of the Fraunhofer ICT and 32nd International Pyrotechnics Seminar*, Karlsruhe, Germany, June 28 – July 1, **2005**, V-13.

[81] C. Walsh, C. Knott, Gun Propellants with FOX-7 and FOX-12, *Dinitramide and FOX-7 Seminar*, April 12–13, **2005**, Karlskoga, Sweden.

[82] C. J. Campagnuolo, C. M. Michienzi, E. G. Tersine, C. D. Knott, W. J. Andrews, IM Solutions of projectiles crimped to cartridges for artillery application – Phase II, *NDIA, IMEMTS Symposium*, 11–14 May **2009**.

[83] M. H. Mason, *Low Temperature Clean Burning Pyrotechnic Gas Generators*, US7,857,920B1, USA, **2010**.

[84] E.-C. Koch, *High Explosives, Propellants, Pyrotechnics*, DeGruyter, Berlin, Boston, **2021**, 369–372; 304–305.

[85] E.-C. Koch, V. Weiser, R. Webb, *O-138 Review on Thermochemical Codes*, Munitions Safety Information Analysis Center, NATO, Brussels, February **2011**, 37 pp.

[86] *STANAG 4115 (Ed.2) Definition and Determination of Ballistic Properties of Gun Propellants*, Military Agency for Standardization (MAS), Brussels, 30 June **1997**, 17 pp.

[87] E. Freedman, Thermodynamic Properties of Military Gun Propellants in L. Stiefel (Ed.) *Gun Propulsion Technology*, Vol. 109 of M. Summerfield (Ed.) Progress in Astronautics and Aeronautics, Washington, **1988**, p. 103–132.

[88] J. A. Vanderhoff, Spectral Studies of Propellant Combustion: Experimental Details and Emission Results for M-30 Propellant, *BRL-MR-3714*, Ballistic Research Laboratory Aberdeen Proving Ground, MD, December **1988**, 21 pp.

[89] W. Langlotz, On the Combustion Behaviour of Heterogeneous Gun Propellants, *IMEMTS*, October 8–11, Bordeaux, France, **2001**.

[90] B. Wang, X. Liao, Z. Wang, L. T. DeLuca, Z. Liu, W. He, Effects of particle size and morphology of NQ on thermal and combustion properties of triple-base propellants, *Combust. Flame*, **2018**, *193*, 123–132.

[91] A. Birk, M. Del Guercio, A. Kinkennon, D. E. Kooker, P. Kaste, Interrupted-Burning Test of Plasma-Ignited JA2 and M30 Grains in a Closed Chamber, *Propellants Explos. Pyrotech.* **2000**, *25*, 133–142.

[92] R. R. Sanghavi, A. G. S. Pillai, S. P. Velapure, A. Singh, Studies on Different Types of Nitrocellulose in Triple Base Gun Propellant Formulations, *Energ. Mater.* **2003**, *21*, 87–95.

[93] A. R. Rye, R. H. Weldon, Sources of Error in High Pressure Strand Burners, *9th Int. Symp. Ballistics*, 29–20 April **1986**, RMCS, Shrivenham, 1–179–1–85.

[94] D. Müller, Procedures for the production of gun propellants by use of different extruders, *J. Haz Mater.* **1983**, *7*, 169–186.

[95] G. O. Nevstad, *Characterization of propellants used in small caliber munitions, FFI/Rapport-2000/02047*, Godkjent, 7 April 2000, 35 pp.

[96] K. Zimmermann, F. Seiler, V. Schlett, F. Schedlbauer, Influence of normal and LOVA Propellant Charges on 20 mm Gun tube Erosion, *12th International Symposium on Ballistics, San Antonio*, Volume II, **1990**, 98–107.

[97] F. Seiler, K. Zimmermann, F. Schedlbauer, *Erosion in a 20 mm-gun produced by normal and LOVA propellant charges, ISL-CO 215/1989*, Institut franco-allemand de recherches de Saint-Louis, **1989**, 34 pp.

[98] B. Baschung, D. Grune, G. Pauly, C. Reynaud, S. Schaefer, French and German test methods to characterize low sensitive gun propellants, *Int. J. Energ. Mater. Chem. Prop.* **2007**, *6*, 269–287.

[99] J. Dahlberg, New Low-Sensitivity Modular Charge Propellant based on GUDN, *IMEMTS* **2006**, Bristol, UK.

[100] J. A. Vanderhoff, Spectral Studies of Solid Propellant Combustion: II. Emission and Absorption Results for M-30 and HMX1 Propellants, *BRL-TR-3055*, Ballistic Research Laboratory Aberdeen Proving Ground, MD, October **1989**, 62 pp.

[101] J. A. Vanderhoff, Species Profiles in Solid Propellant Flames Using Absorption and Emission Spectroscopy, *Combust. Flame* **1991**, *84*, 73–92.

[102] W. R. Anderson, M. S. Miller, Model for Combustion of Triple-Base Propellant with detailed chemistry, *24th Army Science Conference*, 29 November – 2 December **2005**, Orlando, FL, USA.

[103] J. K. Salo, A. J. Bracuti, ARDEC Laboratory Flash Studies, *Proc. Workshop on the Chemical Suppression of Rocket Afterburning and of Gun Muzzle Flash*, Aberdeen, MD, USA, March **1987**, 219–227.

[104] M. S. Miller, Thermal Conductivities and Diffusivities of Solid Gun Propellants, *Combust. Sci. and Tech.* **1994**, *100*, 345–354.

[105] M. S. Miller, Specific heats of solid gun propellants, *Combust. Sci. and Tech.* **1994**, *102*, 273–281.

[106] *NATO Standard, AEP-97, Multi-Calibre Manual of Proof and Inspection (M—CMOPI) for NATO small Arms Ammunition, Volume 16, Barrel Erosion Test Procedure, Ed. A Ver. 1*, NATO Standardization Office (NSO), Brussels, **2019**.

[107] GE/UK/US International Test Operations Procedure (ITOP) 3–2-829, *Cannon Safety Test*, **2003**.

[108] B. Baschung, D. Hensel, D. Grune, A Survey of the Combustion Behavior of Heterogeneous Mixtures Containing Different Inert and Energetic Materials, *35th International Annual Conference of the Fraunhofe rICT*, June 29- July 2, **2004**, Karlsruhe, Germany, V-25.

[109] J. Dahlberg, GUDN propellants and the Uniflex 2 IM Modular Charge System, *36th International Annual Conference of the Fraunhofer ICT,* Karlsruhe, Germany, June 28 – July 1, **2005**, V13.

© 2021 Wiley-VCH GmbH

[110] A. C. Hordijk, O. Leurs, Gun Barrel Erosion – Comparison of Conventional and LOVA Gun propellants, *Transactions ASME*, **2006**, *128*, 246–250.
[111] A. C. Hordijk, C. A: von Driel, M. J. G. Bakker, Propellants and propellant erosivity, *23rd Int. Ball. Symp.*, 16–20 April **2007**, Taragona, Spain, 449–456.
[112] B. Lawton, Thermo-chemical erosion in gun barrels, *Wear*, **2001**, *251*, 827–838.
[113] J. V. R. Kaufman, The effect of nuclear radiation on explosives, *Proc. Roy. Soc.* **1958**, *246*, 219–225.
[114] H. Rosenwasser, Effects of Gamma Radiation on Explosives, *ORNL-1720 Chemistry*, Oak Ridge National Laboratory, November **1955**, 35 pp.
[115] M. A. Bohn, NC-based energetic materials – stability, decomposition, ands ageing, *Nitrocellulose Meeting*, 24–27 April **2007**, Aldermaston, UK.
[116] M. A. Bohn, H. Pontius, Thermal Behaviour of Energetic materials in Adiabatic Self Heating Determined by ARCTM, *43th International Annual Conference of Fraunhofer ICT*, June 26–29, Karlsruhe, Germany, **2012**, V-57.
[117] H. Liu, A. Zhang, R. Fu, A study of the thermal stabilities of nitramine propellants by pyrolysis gas chromatography, *Thermochim. Acta* **1991**, *191*, 131–134.
[118] J. J. Mullay, R. A. Johnson, J. F. Van Norman, Novel Stabilizing Materials for AP Mixtures, *25th International Annual Conference of ICT*, June28 – July 1, **1994**, Karlsruhe, Germany, P-110.
[119] G. M. Low, V. E. Howry, *Hydrazinium nitroformate propellant stabilized with nitroguanidine*, US-Patent 3,658,608, USA, **1972**.
[120] M. B. Talawar, A. Singh, N. H. Naik, B. G. Polke, G. M. Gore, S. N. Asthana, B. R. Gandhe, Effect of organic additives on the mitigation of volatility of 1-nitro-3,3'-dinitroazetidine (TNAZ): Next-generation powerful melt cast able high energy material, *J. Haz. Mater.* **2006**, *A134*, 8–18.
[121] J. J. Mullay, R. A. Johnson, J. F. Van Norman, *Stabilized Munitions containing a NENA Compound*, US-Patent 5,507893, USA, **1996**.
[122] H. F. Hayden, Complex Processes Associated with the Decomposition of N-Guanylurea Dinitramide (FOX-12) and RDX, *Vth Dinitramide and FOX-7 Seminar*, September 21–22, **2011**, Paris, France.
[123] C. W. Fong, R. C. Warren, An Interphasic Region between Nitrocellulose and Nitroguanidine in Triple Base Propellant, *Propellants Explos. Pyrotech.* **1985**, *10*, 69–73.
[124] R. Yazici, D. M. Kaylon, D. Fair, Microstructure and Mixing Distribution Analysis in M30 Triple Base Propellants, *ARWEC-CR-98015*, September **1998**, Picatinny Arsenal, NJ, USA, 37 pp.
[125] C. W. Fong, R. C. Warren, The effect of filler particle size and orientation on the impact fracture toughness of a highly filled plasticized polymeric material, *J. Mater. Sci.* **1985**, *20*, 3101–3110.
[126] R. C. Warren, Dynamic Mechanical and Fracture properties of some double and triple base gun propellants, *MRL-TR-93-40*, Materials Research Laboratory, Maribyrnong, Australia, March **1994**, 36 pp.
[127] C. W. Fong, Crack Initiation in Perforated Propellants under High Strain Rate Impact Conditions, *Propellants Explos. Pyrotech.* **1985**, *10*, 91–96.
[128] C. E. Johnson, P. F. Dendor, No-Roll Process for Manufacture of Double-Base and Composite-Modified Double Base Extrusion Compositions, *Joint Symp. Compatibility of Plastics/Materials with Explosives - Processing Explosives*, May 15–17, **1979**, Albuquerque, NM, USA, 89–99.
[129] P. Della Pieta, C. Vella, Gun Propellant Ignition, *EUROPYRO 2011*, 17–19 May **2011**, Reims, France, 663–669.
[130] W. H. Andersen, Projectile Impact Ignition Characteristics of Propellants, *Report No. 3420-F*, US Army Research Office, May **1980**, 25 pp.
[131] W. H. Andersen, L. J. Irwin, N. A. Louie, Projectile Impact Ignition Characteristics of Propellants II. Single, Double and Triple Base Propellants, *Combust Sci. and Tech.* **1979**, *20*, 1–4.
[132] R. B. Frey, Pressure Measurements in Lightly Confined M456 Cartridge Cases After Primer and Cookoff Ignition, *Ballistic Research Laboratory Memorandum Report, No. 2764*, Ballistics Research Laboratory, Aberdeen, MD, USA, June **1977**.
[133] J. J. Rocchio, R. A. Wires, A Study of the thermal initiation, cookoff, of M30 propellants, *Memorandum Report ARBRL-MR-02847*, Ballistics Research Laboratory, Aberdeen, MD, USA, June **1978**, 39 pp.
[134] T. T. Nguyen, P. Berry, The hot fragment conductive ignition test for screening LOVA propellants, *MRL-TN-661*, Materials Research Laboratory, Adelaide, Australia, March **1994.**
[135] M. S. Kirshenbaum, L. Avrami, B. Strauss, Sensitivity Characterization of Low Vulnerability (LOVA) Propellants, *J. Ballist.* **1983**, *7*, 1701–1740.
[136] V. M. Boyle, The Hugoniots of M-30 propellant and an inert simulator of M-30, *BRL-TR-2684*, October **1985**, 26 pp.
[137] J. N. Majerus, A. B. Merendino, Observations of Shaped-Charge Jet/M30 Propellant reactions, *ARBRL-TR-02108*, September **1978**, Picatinny Arsenal, NJ, USA, 114 pp.
[138] C. Michienzi, C. Knott, Insensitive Propellants for Navy and SOCOM Gun Systems, PARARI **2011**.
[139] G. Petino, W. Seals, R. Rindner, Dust explosion sensitivity tests on M-1, M-30, Comp B and HMX, *ARLCD-CR-79011*, June **1979**, Picatinny Arsenal, NJ, USA, 76 pp.
[140] G. R. Kurulkar, R. K. Syal, H. Singh, Combustible Cartridge Case Formulation and Evaluation, *J. Energ. Mater.* **1996**, *14*, 127–149.
[141] B. Ashcroft, P. Braithwaite, A. Sanderson, T. Manning, R. Marchak, Combustible Cartridge Cases from Energetic Synthetic Polymers, *33rd International Annual Conference of the Fraunhofer ICT*, 25–28 June **2002**, Karlsruhe, Germany, V44.
[142] M. Hund, F. Schedlbauer, Interior Ballistics Investigations of Nitramine Propellants (LOVA), *8th International Symposium on Ballistics*, Orlando FL, USA, October 23-25, **1984**, II-21-II-26.

Manuscript received: September 4, 2020
Revised manuscript received: November 15, 2020
Version of record online: January 20, 2021

 © 2021 Wiley-VCH GmbH